(Accepted version, post peer review and revisions)

Contrasting behaviours of CO_2, S, H_2O and halogens (F, Cl, Br, I) in enriched-mantle melts from Pitcairn and Society seamounts

Mark A. Kendrick[1,2*], Matt Jackson[3], Adam J.R. Kent[4], Erik Hauri[5], Paul J. Wallace[6], Jon Woodhead[1]

1 – School of Earth Science, University of Melbourne, Victoria 3010, Australia.

2 - Research School of Earth Sciences, The Australian National University, Canberra, ACT 0200, Australia.

3 – Department of Earth Science, University of California Santa Barbara, CA 93106-9630, USA

4 – College of Earth, Ocean, and Atmospheric Sciences, Oregon State University, OR 97330, USA

5 – Department of Terrestrial Magnetism, Carnegie Institute of Washington, DC 20015, USA

6 – Department of Geological Sciences, Oregon University, OR 97403, USA

*Corresponding author: mark.kendrick@anu.edu.au

20 ***Words – 5870***

21 **Abstract.**

22 In order to improve characterisation of volatiles in the EM1 and EM2 mantle sources, which
23 are interpreted to contain subducted sedimentary or lithospheric components, we report
24 electron microprobe, FTIR and SIMS CO_2, H_2O, S, F and Cl concentrations of variably
25 enriched glasses from Pitcairn and Society seamounts in Polynesia. The analyses
26 complement previously published Cl, Br and I data for some of the same glasses and all the
27 techniques show reasonable agreement of better than 5-9 % for S, Cl and H_2O. The
28 concentrations of H_2O and all the halogens increase as a function of melt evolution with the
29 highest values of 1.6 wt % H_2O, 2100 ppm F, 1500 ppm Cl, 3.7 ppm Br and 80 ppb I in melts
30 with <2 wt % MgO. In contrast, CO_2 and S are strongly influenced by degassing and it is the
31 least evolved melts that preserve the highest CO_2 concentrations that indicate CO_2
32 oversaturation of some lavas. Comparison of volatile and non-volatile elements of similar
33 compatibility (e.g. H_2O/Ce, Cl/K) as a function of equilibration depth and $^{87}Sr/^{86}Sr$, suggests
34 H_2O and halogens were not significantly degassed from melts equilibrated at >150 bars and
35 most of the variation in H_2O/Ce reflects source variation. Despite their overall enrichment in
36 volatiles, both the Pitcairn and Society EM1 and EM2 sources are depleted in H_2O as well as
37 Cl, Br, and I relative to Ce and K. Slightly different behaviour is suggested for F and a
38 correlation between F/Cl and K/Cl in Pitcairn melts, could be explained by preferential
39 subduction of F relative to Cl into the EM sources. The relative abundances of H_2O,
40 halogens and lithophile elements in melts from different tectonic settings indicate subduction-
41 related H_2O and Cl loss efficiencies are similar at ~90-96%; however, we suggest a lower
42 efficiency for F loss and higher efficiencies for Br and I loss. Nonetheless, dehydrated
43 lithosphere containing 5-10% of its original volatile content is interpreted as the most likely
44 source of volatile enrichment in the Pitcairn and Society mantle sources.

1. Introduction

The geochemistry of seafloor basalts indicates considerable heterogeneity in the Earth's mantle (e.g. Zindler and Hart, 1986; Hofmann, 2003; White, 2010; Stracke, 2012). The magmas produced in intra-plate settings at oceanic islands are commonly enriched in incompatible trace elements, and have more variable Sr, Nd, Pb and He isotope signatures than mid-ocean ridge basalts (MORB) (e.g. Hofmann, 2003; Graham, 2002). Intra-plate Ocean Island Basalts (OIB) characterized by $^{3}He/^{4}He$ ratios of higher than typical MORB (e.g. Hawaii or Iceland) are thought to sample relatively primitive unprocessed mantle material (e.g. Graham, 2002; Jackson et al., 2010; Kurz et al., 1982; Mukhopadhyay, 2012). In contrast, OIB with low $^{3}He/^{4}He$ and radiogenic Sr or Pb signatures (e.g. St Helena, Cook-Australs, Canary Islands) are thought to sample recycled sediment and/or lithospheric materials that have been subducted into the mantle over periods of more than two and a half billion years (Cabral et al., 2013; Graham, 2002; Hanyu et al., 2011; Hofmann, 2003; Hofmann and White, 1982; Parai et al., 2009). A recycled origin can explain the radiogenic Pb or Sr signatures and low $^{3}He/^{4}He$ ratios of OIB that are enriched with incompatible elements, because radiogenic isotopes like ^{87}Sr, ^{206}Pb and ^{4}He would have high abundances in ancient recycled crustal materials with relatively high concentrations of incompatible trace elements such as Rb, Th and U relative to Sr and He (Hilton and Porcelli, 2013; Hofmann, 2003; Plank and Langmuir, 1998). However, some OIB have high or variable $^{3}He/^{4}He$ (and primitive Ne isotope signatures) together with radiogenic Sr signatures (e.g. Pitcairn, Society, Samoa) that suggest they sample a combination of both primitive and recycled mantle materials (e.g. Farley et al., 1992; Honda and Woodhead, 2005; Jackson et al., 2007; Staudacher and Allegre, 1989).

The interpretation that enriched OIB sample recycled sedimentary or lithospheric components means OIB can provide important information about long term geochemical

70 cycling of volatiles and other less-well-constrained elements, that complement the
71 information available from magmas generated in modern arc and back arc settings (e.g.
72 Hofmann, 2003; Stracke, 2012). The fate of volatiles in subduction zones is a subject of
73 ongoing debate (e.g. Dixon et al., 2002; Holland and Ballentine, 2006; Hilton et al., 2002; Ito
74 et al., 1983; Jacobsen and van der Lee, 2006; Kendrick et al., 2011; Parai and
75 Mukhopadhyay, 2012; Rüpke et al., 2004; Wallace, 2005). Sediments and hydrated oceanic
76 lithosphere entering subduction zones have relatively high concentrations of volatile species
77 such as H_2O, halogens, S, CO_2 and atmospheric noble gases (Alt and Honnorez, 1984; Alt
78 and Teagle, 2003; Ito et al., 1983; Staudacher and Allegre, 1988; Kendrick et al., 2011;
79 2013b). However, volatiles are potentially decoupled from subducting slabs by subduction-
80 related metamorphism and devolatilisation that causes fluid loss (Staudacher and Allegre,
81 1988; Hilton et al., 2002; Fischer, 2008), and explain the high H_2O/Ce and Cl/K of magmas
82 in arc and back arc settings (e.g. Kent et al., 2002; Sinton et al., 2003; Wallace et al., 2005;
83 Plank et al., 2013). Alternatively, experimental studies have shown that significant water can
84 be stored in nominally anhydrous minerals formed during slab dehydration (e.g. Kohlstedt et
85 al., 1996; Smyth et al., 2006), meaning that a portion of the water entering subduction zones
86 could be cycled deeply into the Earth's mantle (e.g. Jacobsen and van der Lee, 2006).

87 The fate of water in subduction zones has profound consequences for the geochemical
88 cycles of other trace volatiles and fluid mobile elements. Hydrous minerals are important
89 hosts for halogens and chemically inert noble gases (Jackson et al., 2013; Kendrick et al.,
90 2011). Furthermore, the transport of any fluid mobile element is intrinsically linked to that of
91 water: if significant water is trapped in nominally anhydrous minerals and transported into
92 the deep mantle it implies that this water is unable to advect fluid mobile trace volatiles away
93 from the subducting slab (Kendrick et al., 2011; 2013b).

Submarine glasses from the Pitcairn and Society seamounts of Polynesia are ideal for further evaluating the well-known volatile enrichment of OIB (e.g. Schilling et al., 1980; Jambon and Zimmerman, 1990; Dereulle et al., 1992), because they have extremely variable radiogenic isotopic compositions that extend from enriched compositions that exemplify the so called EM1 and EM2 mantle end-members to an end-member that is close to the MORB mantle or FOZO (Fig 1; Devey et al., 1990; Woodhead and Devey, 1993). Pitcairn is dominated by MORB-like helium with the most primitive neon signatures associated with the EM1 end-member (Fig 5 of Honda and Woodhead, 2005). Nonetheless, the geochemically enriched isotopic signatures of the EM1 and EM2 end-members are usually ascribed to the presence of recycled sediments or lithospheric components in the mantle source (Devey et al., 1990; Hofmann, 2003; Jackson et al., 2007; Woodhead and Devey, 1993). Systematic variations between radiogenic isotope ratios such as $^{87}Sr/^{86}Sr$ (or $^{143}Nd/^{144}Nd$) and volatile contents could therefore provide new insights into the extent to which recycled sediments contribute to the volatile enrichment of OIB sources or are dehydrated during subduction (e.g. Dixon et al., 2002; Workman et al., 2006).

It has been demonstrated previously that the EM1 and EM2 mantle end-members sampled by the Pitcairn and Society melts are depleted in Cl relative to K (and other trace elements), but that they have Br/Cl and I/Cl ratios similar to the MORB mantle (Kendrick et al., 2012b; Stroncik and Haase, 2004). The current study builds on this information by documenting the H_2O, F, S and CO_2 contents of the Pitcairn and Society melts. This is significant because the CO_2 and S concentrations can provide constraints on magma degassing, and systematic trends between the other volatiles and Cl could potentially provide new information about their relative devolatilisation efficiencies during subduction and subsequent residence of subducted materials in the mantle.

2. Sampling, methods and standardization

The submarine glasses used in this study have been documented in a number of previous works (e.g. Ackermand et al., 1998; Devey et al., 1990; Honda and Woodhead, 2005; Kendrick et al., 2012b; Woodhead and Devey, 1993). The samples were recovered by dredging active submarine volcanoes in the Pitcairn and Society seamount chains of Polynesia (Fig 2). The samples from the Pitcairn seamounts situated 70-100 km southeast of Pitcairn Island, were recovered during the SO-65 voyage of the German research vessel *F/S Sonne* in 1989 (Fig 2; Stoffers et al., 1990). The Society seamount samples were recovered during cruises of the *N.O. Jean Charcot* and *F/S Sonne* vessels from a series of submarine volcanoes southeast of Tahiti during 1983 and 1987, respectively (Fig 2; Cheminee et al., 1989; Stoffers, 1987).

The Society glasses derive from the flanks of five different volcanoes and therefore represent the volcanic products of several magma chambers. The majority of Pitcairn glasses derive from the Bounty Volcano, but they encompass distal flank areas of the volcano, have different chemistry, and almost certainly represent different magma batches (Fig 2). Collectively the glasses are considered to represent recent expressions of evolving magma chambers fed by the Pitcairn and Society hotspots (Cheminee et al., 1989; Stoffers, 1987; Stoffers et al., 1990; Devey et al., 2003).

Volatiles in 18 Pitcairn and Society glasses selected for this study have been analysed using several complementary techniques: 1) S and Cl were measured along with major elements by Cameca SX-100 electron microprobe at Oregon State University. Complementary trace element analyses were undertaken by laser ablation inductively coupled plasma mass spectrometry at the W.M. Keck Collaboratory for Plasma Spectrometry, Oregon State University. 2) FTIR was used to measure the glass H_2O content at the University of

144 Oregon; and 3) SIMS measurements of H_2O, CO_2, S, F and Cl were obtained using the
145 Cameca IMS 6F ion microprobe at the Department of Terrestrial Magnetism, Carnegie
146 Institute of Washington. In addition, 4) fourteen of the glasses were previously investigated
147 for Cl, Br and I using the noble gas method (Kendrick et al. 2012b), providing a combined
148 dataset for volatiles in 24 glasses.

149 Electron microprobe analysis at Oregon State University used an accelerating voltage
150 of 15 keV and current of 30 nA with counting times optimised for measurement of S (30 s)
151 and Cl (100 s), following the approach of Rowe et al. (2009). Precision is estimated at 12 %
152 (2σ) for Cl based on duplicate analyses of Loihi glass (LO-02-02) that gave 1340 ± 160 ppm
153 Cl compared to ~1390 ppm Cl in a previous study (Kent et al., 1999b). Trace element
154 analyses achieved using the NewWave DUV 193 Excimer laser and VG PQ Excell
155 quadrupole ICP-MS followed the techniques reported in Kent et al. (2004). Individual
156 analyses used a spot of between 50-80 μm diameter and a pulse rate of 4 Hz. The reported
157 concentrations represent the averages of 3-5 measurements made using BCR-2G as the
158 calibration standard and electron microprobe CaO contents. Concentrations determined for
159 BHVO-2G, analysed as an unknown, were within 10% of accepted values. Analogous
160 procedures were used to analyse 5 glasses at the University of Melbourne, for which only Cl,
161 Br and I volatile data were available.

162 Dissolved H_2O was measured by FTIR using a ThermoNicolet Nexus 670
163 spectrometer and Continuum microscope at the University of Orgeon. Doubly polished
164 wafers of each glass were prepared for analysis, with the thicknesses measured by digital
165 micrometer. Total H_2O concentrations were determined using the OH stretching vibration at
166 3560 cm^{-1} and an absorption coefficient of 63 L/mol cm (Dixon et al., 1995). The accuracy
167 of FTIR H_2O measurements on basalt glasses is commonly estimated as ±10% (e.g. Dixon
168 and Clague, 2001). The absorption coefficinet for the OH stretching vibration is relatively

169 constant over a wide range of basaltic to andesitic compositions (Dixon and Clague, 2001;
170 King et al., 2002; Mandeville et al., 2002); however, the choice of absorption coefficient
171 represents an additional uncertainty for evolved alkaline glasses.

172 SIMS analysis used a focussed primary Cs^+ ion beam (10-15 nA) rastered over a
173 40×40 μm area on the glasses, with a field aperture selected to mask emission from the crater
174 edge and extract ions from only the central 10μm of the sputter crater. The entrance and
175 detector slits were arranged to give sufficient mass resolution (4500) to resolve known
176 volatile interferences, mainly ^{17}O on ^{16}OH, ^{18}OH on ^{19}F, and $^{16}O_2$ on ^{32}S. Counting times of
177 10s were employed for ^{12}C and 2s for the remaining isotopes ^{16}OH, ^{19}F, ^{32}S and ^{35}Cl and the
178 normalizing isotope ^{30}Si. The reported concentrations represent the averages of 3-5
179 individual measurements on each glass, standardized against a suite of 45 basaltic and
180 andesitic glasses for volatile abundances, following methods detailed in Hauri et al. (2002,
181 2006).

182 Finally, the concentrations of halogens and K previously reported by Kendrick et al
183 (2012b) were based on irradiation-produced noble gas proxy isotopes measured relative to an
184 air standard, and converted to Cl, Br, I and K via production ratios monitored with mineral
185 standards (Kendrick, 2012). This methodology normally provides very high internal
186 precision of 2-4 % (2σ) for concentration and ratio measurements; however, changes in the
187 Br and I abundances recommended for the scapolite standards (see Kendrick et al., 2013ab),
188 require that the previously reported concentrations are reduced by 20 % for Br and 25 % for I.
189 Revising the Br and I concentrations does not change the conclusions of the previous study,
190 which were based on an internally consistent dataset (Kendrick et al., 2012ab); however, it
191 will facilitate future comparison between laboratories and Br or I measurements made by

192 different techniques. The basis of the monitor re-calibration is described in detail by
193 Kendrick et al. (2013a).

194

195 **3. Results**

196 The new electron microprobe, FTIR and SIMS Cl, F, H_2O, CO_2 and S data are
197 reported in Tables 1 and 2 together with selected major and trace elements, key isotopic ratios
198 from previous studies (Devey et al., 1990; Woodhead and Devey, 1993; Honda and
199 Woodhead, 2005; Staudacher and Allegre, 1989) and revised Br and I concentration data
200 from Kendrick et al. (2012b). The full electron microprobe and laser ablation ICPMS
201 datasets, including standard analyses, are available in the electronic supplement.

202 The most primitive glasses have 6-7 wt. % MgO and 45-49 wt % SiO_2, whereas the
203 most evolved glasses have 1-2 wt % MgO and 55-65 wt % SiO_2 (Fig 3; Tables 1 and 2).
204 The SiO_2, Na_2O and K_2O concentrations of the glasses (Supplementary Data) encompass
205 basanites, alkali basalts, trachy-basalts, trachy-basaltic andesites and trachytes, with the
206 Society glasses recording the most evolved major element compositions (Fig 3)). This large
207 range of melt compositions is a consequence of our sampling strategy, because some of the
208 isotopically most enriched samples represent early-formed highly differentiated melts
209 dredged from small seamounts (Fig 3c; Devey et al., 2003). Note that halogen measurements
210 were conducted on a very small piece of CH DR1 P1-1 glass (e.g. ~0.7 mg; Kendrick et al.,
211 2012b), and while major and trace element data are not available for this glass (Table 2),
212 whole rock data indicate a basanitic composition with 7.8 wt % MgO and 45 wt % SiO_2
213 similar to the least evolved glasses from Society (Fig 3; Devey et al., 1990).

214 The different techniques used to measure H_2O, Cl and S yield very similar results
215 indicating the glasses have 0.75 to 1.6 wt. % H_2O; 480 to 2090 ppm F, 200 to 1450 ppm Cl;
216 250-3700 ppb Br, 21-77 ppb I, 2.3 to 160 ppm CO_2 and 240 to 2500 ppm S (Fig 4; Tables 1
217 and 2). In general, the highest concentrations of H_2O and halogens occur in the most evolved
218 melts, whereas CO_2 and S have lower concentrations in the more evolved melts (below;
219 Table 1 and 2).

220 The average discrepancies between the techniques are less than 5-6 % for Cl and S
221 and 9% for H_2O (Fig 4). The discrepancy between SIMS and FTIR H_2O is largest for the
222 more evolved glasses; however, the average discrepancy is similar to the accuracy of these
223 techniques. As a result we believe that our interpretations are not influenced by inter-
224 laboratory biases and standardization summarised in section 2 is not discussed further in this
225 contribution.

226 In the discussion below we use SIMS data for H_2O, CO_2, S and F; and Br and I
227 concentrations determined by the noble gas method. Chlorine concentrations are based on
228 either the noble gas method, electron microprobe or SIMS data, such that both elements in
229 any ratio have been measured by the same technique. This avoids introducing small biases
230 related the analysis of different sample aliquots.

231

232 **4. Discussion**

233 Before considering how the volatile content of the Pitcairn and Society melts could be related
234 to subduction-recycling processes, we first evaluate the extent to which volatiles have been
235 modified by shallow level processes occurring during magma residence in the crust or
236 eruption. In addition to fractional crystallisation, two shallow level processes that have the
237 potential to strongly alter the glasses volatile content are degassing and seawater assimilation.

238

239 *3.1 Volatile degassing*

240 The Pitcairn and Society glasses included in this study have vesicles ranging from
241 micrometres to millimetres in diameter that are estimated to occupy between ~5 and 30 vol.
242 % of some glasses (Table 3; Ackermand et al., 1998; Aubaud et al., 2005; 2006; Hekinian et
243 al., 1991). Furthermore some of the Society samples were reported to be popping rocks that
244 released the smell of H_2S immediately after dredging (Hekinian et al., 1991), and Ackermand
245 et al. (1998) estimated that sulphides coating the inside surfaces of vesicles in Pitcairn
246 samples 52DS-1 and 57DS-1 accounted for up to ~1 vol. % of the glass. These observations
247 suggest the melts degassed substantial CO_2 and variable quantities of S (Ackermand et al.,
248 1998; Hekinian et al., 1991), as well as limited H_2O, which is present in the vesicles (Aubaud
249 et al., 2005; 2006).

250 Volatile solubility is pressure dependent and solubility models developed from
251 experimental data can be used to calculate equilibrium degassing pressures based on the
252 measured H_2O and CO_2 concentrations (e.g. Dixon et al., 1995; Iacono-Marziano et al.,
253 2012). However, in addition to the pressure effect, CO_2 solubility is strongly dependent on
254 melt composition with CO_2 solubility enhanced by high CaO, K_2O and Na_2O in mafic
255 magmas or the presence of H_2O, and reduced by SiO_2 in more evolved melts (e.g. Dixon et
256 al., 1995; Dixon, 1997; Iacono-Marziano et al., 2012). The solubility of H_2O is less sensitive
257 to composition than CO_2, but H_2O is significantly more soluble in trachytic melts than in
258 rhyolitic magmas (Di Matteo et al., 2004).

259 The SIMS CO_2 and H_2O concentration data have been modelled in Fig 5 using the
260 VolatileCalc program (Newman and Lowenstern, 2002) which is based on the solubility
261 model of Dixon et al., (1995) and Dixon (1997). Newman and Lowenstern (2002) indicated

262 that VolatileCalc can be used to model mafic compositions in the tholeiite to nephelinite
263 range, including the alkali basalts and basinites relevent to this study (Fig 3). However, the
264 SiO_2 input parameter is limited to the range 40-49 wt. % and the results are questionable for
265 melts with >52 wt % SiO_2 (Newman and Lowenstern, 2002). Despite this limitation, the
266 Pitcairn glasses with SiO_2 of 49.1-55.7 wt % lie close to the equilibrium line in Fig 6b, and
267 taken at face value, the volatile concentrations in these melts appear to have been closely
268 equilibrated to the depth of eruption (Fig 6).

269 The Society glasses encompass a greater range of compositions than the Pitcairn
270 glasses and the most evolved melts with more than 60 wt % SiO_2 (Fig 3) were modelled as
271 rhyolites rather than basalts in VolatileCalc (Fig 6b). The apparent understaturation of some
272 of the melts could be related to the limitations of the solubility model; however, two of the
273 Society glasses with <49 wt % SiO_2 are indicated to be significantly over-saturated with
274 respect to CO_2 (Fig 6b). A similar degree of oversaturation is also suggested for these glasses
275 by an alternative solubility model developed for alkaline magmas (Table 2; Iacono-Marziano
276 et al., 2012); and in contrast to VolatileCalc this model suggests the Pitcairn glasses could be
277 similarly oversaturated with respect to CO_2 and H_2O (Table 1). Oversaturation of submarine
278 melts with respect to CO_2 is commonly observed on many mid-ocean ridges and is usually
279 interpreted to indicate that although some degassing has occurred, its efficiency was limited
280 by a rate of magma ascent greater than the rate of CO_2 diffusion into vesicles (e.g. Chavrit et
281 al., 2012; Dixon and Stolper, 1995; Pichavant et al., 2013).

282 The relative importance of degassing is much greater for CO_2 than H_2O or halogens
283 which have relatively high solubilities in silicate melts (Dixon et al., 1995; Dixon 1997;
284 Webster et al., 1999). The two Society samples in this study that were investigated by
285 Aubaud et al. (2005), can be estimated to contain 95-97% of their total CO_2 in vesicles
286 compared to only 10-20 % of their total H_2O (Table 3). However, the significance of these

287 numbers depends on the relationship between the vesicles and matrix glass: if vesicles were
288 lost from the melt prior to quenching these figures would represent minimums for CO_2 and
289 H_2O degassing, but if the vesicles were derived from a volume of melt larger than the sample,
290 they could overestimate the extent of degassing. We favour the latter interpretation because
291 while matrix CO_2 concentrations show a pronounced decrease toward the more evolved
292 compositions, that is consistent with the expected enhanced degassing of CO_2 in SiO_2-rich
293 melts (Fig 6a), the data in Table 3 would suggest the basanitic sample (CH DR1 P3-4) was
294 degassed more efficiently than the trachytic sample (CH DR4 4-1). Sulphur and Cu show a
295 decrease with melt evolution similar to CO_2 (Fig 6a); however, this is related to a
296 combination of S degassing and crystallisation of sulphide phases, given that sulphides are
297 present in the ground mass as well as within vesicles of the most evolved rocks (Ackermand
298 et al., 1998). In contrast to CO_2 and S, H_2O increases during melt evolution, in a manner that
299 is similar to the halogens and other incompatible elements like K that are not significantly
300 degassed or fractionated by sulphides (Fig 6b).

301 The extent to which relatively minor H_2O degassing could contribute to the scatter of
302 H_2O concentrations in the MgO concentration plot is unclear, but these data can be explained
303 by mixing depleted mantle and EM magma components in the majority of samples (Fig 6b).
304 Therefore, in order to further isolate the possible effects of H_2O degassing we examine the
305 concentrations of selected volatiles relative to non-volatile lithophile elements of similar
306 compatibility as a function of eruption depth (Fig 7) and $^{87}Sr/^{86}Sr$ (Fig 8). The logic is that
307 because element pairs of similar compatibility, like CO_2/Nb, H_2O/Ce, Cl/K and F/Nd, are not
308 strongly modified by crystallisation of common silicate minerals (olivine, pyroxene and
309 plagioclase), variation in these ratios is mainly ascribed to either degassing processes or the
310 source composition. Variations caused by degassing should be revealed by a systematic

311 relationship to eruption depth, whereas variations related to source composition may be
312 correlated with $^{87}Sr/^{86}Sr$.

313 As would be expected, the CO_2/Nb ratio decreases with decreasing eruption depth,
314 consistent with strong CO_2 degassing (Fig 7a; S/Dy behaves in a similar way and neither ratio
315 is correlated with $^{87}Sr/^{86}Sr$). In contrast, the H_2O/Ce ratio varies from 60 to 150 in the
316 majority of samples, but a lower value of 43 suggests H_2O degassing was significant for the
317 shallowest samples (Fig 7b). The glasses have fairly constant F/Nd over the entire range of
318 eruption depth (Fig 7c), and both F/Nd and Cl/K of the Pitcairn samples increase toward
319 shallower depths (albeit with significant scatter), which is the opposite to the trends that
320 would result from degassing (Fig 7d). Notice also that the H_2O/Ce ratio of the Pitcairn
321 samples equilibrated at more than 100 bars show a similar increase toward shallower depth
322 (Fig 7b) and both H_2O/Ce and Cl/K are correlated with $^{87}Sr/^{86}Sr$ (Fig 8).

323 These observations are consistent with previous work indicating that halogens are not
324 significantly degassed from melts erupted in water depths of more than ~500 m (Straub and
325 Layne, 2003; Unni and Schilling, 1978) and the relatively high solubility of H_2O in silicate
326 melts (Dixon et al., 1995; Dixon, 1997; Webster et al., 1999). In the ensuing discussion, and
327 based on the information from Fig 7, we therefore assume that none of the melts have lost
328 halogens through degassing and that melts erupted at pressures of >150 bars have retained
329 H_2O concentrations within ~10% of their original values. The suggested preservation of H_2O
330 concentrations close to pre-degassing values is consistent with the melts either having
331 originally had low CO_2 contents, or more likely that CO_2 degassing occurred predominantly
332 in an open system.

333

334 *3.2 Seawater assimilation*

335 Previous work has shown submarine magmas can have elevated Cl concentrations,
336 above what can be explained by fractional crystallisation, as a result of assimilating seawater-
337 derived components (e.g. Kendrick et al., 2013a; Kent et al., 1999ab; 2002; le Roux et al.,
338 2006; Michael and Cornell, 1998; Wanless et al., 2011). However, several lines of evidence
339 suggest the Pitcairn and Society melts have not been significantly influenced by assimilation
340 processes.

341 Firstly, the range of H_2O and Cl concentrations in the melts can be explained by
342 fractional crystallisation and mixing the depleted and enriched magma components (Fig 6b)
343 which are required to explain the range in isotope compositions (Fig 1), and Cl/K does not
344 increase as a function of MgO (Tables 1 and 2; supplementary data Fig S1). The liquid lines
345 of descent in Figs 6b have been calculated with Petrolog3 (Danyushevsky and Plechov, 2011)
346 by progressively crystallising olivine, plagioclase, pyroxene, ilmenite and magnetite and
347 assuming K, H_2O and Cl are all perfectly incompatible. The mineral compositions were
348 evolved during crystallisation according to the mineral models of Arisken et al. (1993),
349 Arisken and Barmina (1999) and Bolikhovskaya et al. (1999). The magma starting
350 compositions at 8 wt % MgO were selected to fit the data and be realistic for MORB and OIB
351 magmas; however, it should be noted that the choice of starting composition and mineral
352 model significantly influences the slope of liquid lines of descent and the models are intended
353 only to be indicative of a melts possible evolution below 4 wt % MgO.

354 Secondly, it has been demonstrated that in every known case where magmas have
355 assimilated seawater-derived Cl, Cl and H_2O were introduced in high salinity brines, leading
356 to strong correlations between H_2O/Cl, Br/Cl, I/Cl, F/Cl and K/Cl (see Kendrick et al., 2013a
357 for a complete discussion). In contrast, these ratios are not systematically correlated between
358 the Society and Pitcairn glasses, which preserve Br/Cl and I/Cl typical of the mantle (Fig 9;
359 Kendrick et al., 2013a). Note that the H_2O/Cl and F/Cl data in Fig 9c do exhibit a weak

360 correlation (r^2 = 0.58); however, this trend cannot be explained by assimilation of seawater
361 components because H_2O/Cl is not similarly correlated with K/Cl (Fig 9a), and Br/Cl is not
362 correlated with either K/Cl or I/Cl (Fig 9).

363 Finally, the glasses from both Pitcairn and Society exhibit relationships between
364 H_2O/Ce and $^{87}Sr/^{86}Sr$, and Cl/K and $^{87}Sr/^{86}Sr$ (Figs 8ac), that would not have been preserved
365 if significant assimilation of seawater-derived components had occurred (seawater $^{87}Sr/^{86}Sr$ =
366 0.709; see Fig 9), or if these melts had lost significant H_2O during degassing.

367

368 *3.3 Volatiles in the Pitcairn and Society EM sources*

369 In the preceding sections we argued Pitcairn and Society melts erupted under water pressures
370 of more than 150 bars preserve H_2O and halogen concentrations of close to their original
371 values. Furthermore, the melts have a limited range of Br/Cl and I/Cl that indicate the
372 behaviours of Br and I are similar to Cl (Figs 8 and 9d; Schilling et al., 1980; Kendrick et al.,
373 2012a; 2013a). In this section we further evaluate variations in the relative concentrations of
374 halogens and H_2O in Pitcairn and Society melts and relate these variations to mixing of
375 depleted and enriched components in the mantle sources (Fig 1).

376 Despite their high volatile contents, the Pitcairn and Society melts have H_2O/Ce,
377 Cl/K, Br/K and I/K ratios, that show marked decreases as a function of mantle enrichment
378 indicated by $^{87}Sr/^{86}Sr$ (Figs 8a,c,e and f; Stroncik and Haase, 2004; Kendrick et al., 2012b).
379 It should be noted that similar trends are obtained if $^{143}Nd/^{144}Nd$ is used in place of $^{87}Sr/^{86}Sr$
380 or La instead of K; and that sample 45-DS-1, believed to have degassed significant H_2O (Fig
381 7b), is not shown in these plots. Fluorine is distinguished from the other halogens and H_2O
382 because in contrast to H_2O/Ce and Cl/K, the F/Nd ratios of the Society and Pitcairn melts are

not strongly correlated with $^{87}Sr/^{86}Sr$ (Fig 8d). Previous studies have demonstrated comparable depletions of H_2O/Ce in enriched mantle sources sampled by the Shona, Discovery and Azores anomalies of the Atlantic, as well as the Kerguelen and Samoan plumes (Dixon et al., 2002; Wallace, 2002; Workman et al., 2006). The lowest Cl/K were also measured in the enriched source of the Kerguelen plume (Wallace, 2002). In contrast, the Cl/K systematics of the Samoan melts were obscured by seawater assimilation (Workman et al., 2006), but the Samoan melts are characterised by a uniform F/Nd of 22 ± 3 (n = 88; 2σ) that does not vary as a function of $^{87}Sr/^{86}Sr$ (Workman et al., 2006; cf. Fig 8d).

The characteristically low H_2O/Ce, Cl/K, Br/K and I/K ratios of the enriched mantle sources investigated (Fig 8; Dixon et al., 2002; Wallace, 2002; Workman et al., 2006) are consistent with the presence of subducted oceanic lithosphere that was efficiently devolatilised during subduction. Dehydrated lithosphere could generate a strong enrichment in incompatible lithophile elements, whereas its volatiles would have been at least partly lost during subduction (e.g. Dixon et al., 2002; Jambon and Zimmerman, 1990; Workman et al., 2006; Kendrick et al., 2012b). In this scenario, the lack of a strong correlation between F/Nd and $^{87}Sr/^{86}Sr$ in the Pitcairn, Society and Samoan melts, which is characteristic of F depletion comparable to the relative depletions of Cl and H_2O (Fig 8d; Workman et al., 2006), could be explained if F was recycled into the enriched mantle sources more efficiently than the heavier halogens and H_2O (Fig 8).

Preferential subduction of F relative to Cl is consistent with the correlation between F/Cl and K/Cl in Pitcairn melts (r^2 = 0.77; Fig 10), which cannot be explained by seawater assimilation (section 3.2; Fig 8d). Furthermore, while detailed studies of F behaviour in subduction zones are rare (John et al., 2011; Portnyagin et al., 2007; Straub and Layne, 2003), preferential subduction of F relative to Cl might be expected to result from the higher compatibility of F in mica and amphibole, and the higher solubility of F in the nominally

anhydrous minerals formed during slab dehydration (Bernini et al., 2013; Beyer et al., 2012; Dalou et al., 2012).

3.4 Comparison with other mantle reservoirs

The relative depletion of H_2O, Cl, Br and I in enriched mantle sources (Fig 9) is consistent with the presence of dehydrated subducted sediments or lithospheric components in the EM sources, but it does not constrain the source of volatiles in the enriched-mantle. In order to provide additional inferences on the sources of volatiles in the EM sources, as well as the efficiency of dehydration, we have compiled data for the relative abundances of K, Ce, F, Cl, Br, I, and H_2O in submarine glasses from different tectonic settings (Table 4). The compiled data have been selected to avoid samples obviously influenced by seawater assimilation, which was evaluated using X/Cl plots similar to Fig 8, enabling analyses representative of the mantle to be selected. A striking feature of the compilation is that the EM1 and EM2 mantle reservoirs have H_2O/Cl, Br/Cl and I/Cl ratios that are very similar to MORB, but based on the limited data available MORB has more variable and sometimes higher F/Cl ratios than the EM mantle reservoirs investigated (Table 4).

The similarity between MORB and OIB Br/Cl, I/Cl and H_2O/Cl ratios is partly explained because these elements have similar compatibilities in the mantle and are not easily modified by melting or fractional crystallisation (Kendrick et al., 2012a; Michael, 1995; Dixon et al., 2002). Recent Cl isotope data have suggested Cl in enriched mantle reservoirs may be distinct to that in MORB (John et al., 2010). However, there is no good reason that primordial and recycled volatiles would have similar H_2O/Cl, Br/Cl and I/Cl ratios, so we interpret the relative uniformity of these abundance ratios to indicate that these volatiles either: i) have a dominantly primordial origin in the mantle, and mantle abundance ratios

have not been disturbed by the introduction of recycled materials; or ii) these volatiles have a dominantly recycled origin throughout the mantle, and their relative abundance ratios are controlled by slab processes.

The suggested association of primitive noble gases with recycled materials in the EM1 end-member of the Pitcairn plume (Honda and Woodhead, 2005) implies H_2O, Cl, Br and I could have either a primordial or recycled origin in the Pitcairn melts. However, the lack of a relationship between $^3He/^4He$ and H_2O/Ce in the Pitcairn samples (Fig 11) and the MORB mantle (Michael, 1995), and the presence of subducted atmospheric noble gases in the convecting mantle (Holland and Ballentine, 2006), is interpreted here to favour a recycled origin for other seawater-derived volatiles like H_2O, Cl, Br, I, throughout most of the mantle.

The low H_2O/Ce (~60-80) and Cl/K (~0.025 (K/Cl = 40)) of the EM sources relative to MORB (H_2O/Ce ~100-300; Cl/K ~0.1-0.05 (K/Cl = 10-20)), can be used together with data from arc-backarc magmas with H_2O/Ce of ~1000-3000 and Cl/K ~1 (Table 4), to estimate the cumulative efficiency of volatile loss during subduction and subsequent residence in the mantle:

$$\% H_2O \text{ loss} = [(H_2O/Ce)_{BABB}-(H_2O/Ce)_{MORB}]/[(H_2O/Ce)_{BABB}-(H_2O/Ce)_{EM}]\times 100$$

$$\% Cl \text{ loss} = [(Cl/K)_{BABB}-(Cl/K)_{MORB}]/[(Cl/K)_{BABB}-(Cl/K)_{EM}]\times 100$$

On this basis, we estimate that both H_2O and Cl are lost from subducted slabs with fairly similar efficiencies of ~90-96 %, a figure that is similar to the H_2O loss efficiency of 92 % previously estimated by comparing sediment and enriched mantle H_2O/Ce ratios (Dixon et al., 2002). The similar efficiencies suggested for H_2O and Cl loss explain why mantle H_2O/Cl varies from only ~10 to ~50 (Table 4), and this ratio does not vary as a function of $^{87}Sr/^{86}Sr$ in our samples (Fig 8b).

In comparison to H_2O and the heavy halogens, the mantle F/Cl ratio is more likely to be disturbed by melting and fractional crystallisation, because F is less incompatible than Cl (Bernini et al., 2013; Beyer et al., 2012; Dalou et al., 2012). The available data indicate MORB has typical F/Cl of ~1-10 (Table 4), which overlaps with what has been reported for EM sources (F/Cl of ~1.5-3; Table 4), but probably also reflects melting and fractionation processes. Despite this complexity, many analyses of arc and backarc lavas have F/Cl <1 that are significantly lower than MORB and OIB F/Cl ratios (Table 4), consistent with F being subducted into the mantle preferentially relative to Cl (Straub and Layne, 2003).

Finally, the high Br/Cl and I/Cl ratios of materials entering subduction zones (Kendrick et al., 2013), and the uniquely high I/Cl of backarc basin basalts compared to MORB and OIB (Table 4), requires that I and Br are preferentially lost from subducting slabs relative to Cl in the early part of the subduction cycle (Kendrick et al., 2011; 2013b). Therefore, the total Br and I loss efficiencies during slab dehydration must be more than the F and Cl loss efficiencies (e.g. >90-96%). However, if halogens in the EM reservoirs have a dominantly recycled origin as suggested, the uniformity of H_2O/Cl, Br/Cl and I/Cl in the MORB and OIB mantle (Table 4) imply that subducted H_2O, Cl, Br and I also dominate the MORB inventory of these volatiles. Furthermore after bypassing the arc, H_2O, Cl, Br and I retained in the dehydrated slab (presumably hosted by fluid inclusions, grain boundaries and nominally anhydrous minerals) are not strongly fractionated from each other during melting reactions and mixing into the mantle. As a result, mineral breakdown reactions during subduction may control the abundance ratios of certain volatiles throughout the entire mantle, thus explaining the lack of a strong enrichment of I relative to other halogens in enriched reservoirs inferred to contain subducted sedimentary components (cf. Dereulle et al., 1992).

5. Conclusions

The Pitcairn and Society melts are strongly enriched in trace elements and volatiles relative to typical mid-ocean ridge basalts. However, the most enriched end-members show depletions in most volatiles relative to lithophile elements of similar compatibility, e.g. the most enriched melts have the lowest H_2O/Ce, Cl/K, Br/K and I/K ratios. Comparison of H_2O/Ce and Cl/K of magmas from different tectonic settings suggests H_2O and Cl are lost from subducted slabs with similar efficiencies of ~90-96%.

The relative uniformity of H_2O/Cl, Br/Cl and I/Cl in enriched mantle reservoirs sampled by OIB, and the MORB mantle (Table 4), suggests subducted volatiles have been mixed throughout the entire mantle. Differences between MORB-OIB melts and melts generated in arc and back arc settings imply a higher subduction efficiency for F than Cl (e.g. F loss efficiency of <90%) and lower subduction efficiencies of Br and I (e.g. Br and I loss efficiencies of >90-96%). However, the uniformity of mantle Br/Cl, I/Cl and H_2O/Cl favours a dominantly recycled rather than primordial origin for these volatiles in the mantle.

Acknowledgements

The samples used in this study were recovered during cruises of the *F/S Sonne and N.O. Jean Charcot* and were funded by German Research Ministry and CNRS (France), respectively. We gratefully acknowledge the senior scientists (P. Stoffers and J.L. Cheminee) and crews of these vessels which made the voyages possible. JDW participated in the 1989 SO-65 cruise to Pitcairn and is endebted to Colin Devey for supplying Society samples to him ~20 years ago as part of a previous study. Alison Koleszar assisted with electron microprobe and LA-ICP-MS analyses. Dr. Adam Kent was supported by NSF grant OCE 1028707, and Dr Matt

503 Jackson was supported by NSF grants OCE-1061134 and EAR-1145202. Dr Mark Kendrick
504 was the recipient of an Australian Research Council QEII Fellowship (project number DP
505 0879451).

506

507 **References**

508 Ackermand, D., Hekinian, R., Stoffers, P., 1998. Magmatic sulfides and oxides in volcanic
509 rocks from the Pitcairn hotspot (South Pacific). Mineralogy and Petrology, 64(1-4):
510 149-162.

511 Alt, J., Honnorez, J., 1984. Alteration of the upper oceanic crust, DSDP site 417: mineralogy
512 and chemistry. Contributions to Mineralogy and Petrology 87, 149-169.

513 Alt, J.C., Teagle, D.A.H., 2003. Hydrothermal alteration of upper oceanic crust formed at a
514 fast-spreading ridge: mineral, chemical, and isotopic evidence from ODP Site 801.
515 Chemical Geology 201, 191-211.

516 Arisken, A.A., Barmina, G.S., 1999. An empirical model for the calculation of spinel-melt
517 equalibria in mafic igneous systems at atmospheric pressures: 2. Fe-Ti oxides.
518 Contributions to Mineralogy and Petrology 134, 251-263.

519 Arisken, A.A., Frenkel, M.Y., Barmina, G.S., Nielsen, R., 1993. COMAGMAT: A
520 FORTRAN program to model magma differentiation processes. Computers &
521 Geosciences 19, 1155-1170.

522 Aubaud, C., Pineau, F., Hékinian, R., Javoy, M., 2005. Degassing of CO2 and H2O in
523 submarine lavas from the Society hotspot. Earth and Planetary Science Letters 235,
524 511-527.

525 Aubaud, C., Pineau, F., Hekinian, R., Javoy, M., 2006. Carbon and hydrogen isotope
526 constraints on degassing of CO2 and H2O in submarine lavas from the Pitcairn
527 hotspot (South Pacific). Geophysical Research Letters 33.

528 Bernini, D., Wiedenbeck, M., Dolejs, D., Keppler, H., 2013. Partitioning of halogens between
529 mantle minerals and aqueous fluids: implications for the fluid flow regime in
530 subduction zones. Contributions to Mineralogy and Petrology, 165(1): 117-128.

Beyer, C., Klemme, S., Wiedenbeck, M., Stracke, A., Vollmer, C., 2012. Fluorine in nominally fluorine-free mantle minerals: Experimental partitioning of F between olivine, orthopyroxene and silicate melts with implications for magmatic processes. Earth and Planetary Science Letters, 337–338(0): 1-9.

Bolikhovskaya, S.V., Vasil'eva, M.O., Koptev-Dvornikov, E.V., 1995. Modelling of low Ca-pyroxene crystallisation in basic systems (New versions of geothermometers). Geokimia 12, 1710-1727.

Cabral, R.A., Jackson, M.G., Rose-Koga, E.F., Koga, K.T., Whitehouse, M.J., Antonelli, M.A., Farquhar, J., Day, J.M.D., Hauri, E.H., 2013. Anomalous sulphur isotopes in plume lavas reveal deep mantle storage of Archaean crust. Nature 496, 490-493.

Chavrit, D., Humler, E., Morizet, Y., Laporte, D., 2012. Influence of magma ascent rate on carbon dioxide degassing at oceanic ridges: Message in a bubble. Earth and Planetary Science Letters 357–358, 376-385.

Cheminee, J.L., Hekinian, R., Talandier, J., Albarede, F., Devey, C.W., Francheteau, J., Lancelot, Y., 1989. Geology of an active Hot Spot - Teahitia-Mehetia region in the South Central Pacific. Marine Geophysical Researches 11, 27-+.

Dalou, C.l., Koga, K., Shimizu, N., Boulon, J., Devidal, J.-L., 2012. Experimental determination of F and Cl partitioning between lherzolite and basaltic melt. Contributions to Mineralogy and Petrology: 1-19.

Danyushevsky, L.V., Plechov, P., 2011. Petrolog3: Integrated software for modeling crystallization processes. Geochemistry, Geophysics, Geosystems 12, Q07021.

Deruelle, B., Dreibus, G., Jambon, A., 1992. Iodine abundances in oceanic basalts: implications for Earth dynamics. Earth and Planetary Science Letters 108, 217-227.

554 Devey, C.W., Albarede, F., Cheminee, J.L., Mischard, A., Muhe, R., Stoffers, P., 1990.
555 Active Submarine Volcanism on the Society Hotspot Swell (West Pacific): A
556 Geochemical Study. Journal of Geophysical Research 95, 5049-5066.
557 Devey, C.W., Lackschewitz, K.S., Mertz, D.F., Bourdon, B., Cheminee, J.L., Dubois, J.,
558 Guivel, C., Hekinian, R., Stoffers, P., 2003. Giving birth to hotspot volcanoes:
559 Distribution and composition of young seamounts from the seafloor near Tahiti and
560 Pitcairn islands. Geology 31, 395-398.
561 Dixon, J.E., 1997. Degassing of alkalic basalts. Am. Miner. 82, 368-378.
562 Dixon, J.E., Clague, D.A., 2001. Volatiles in basaltic glasses from Loihi seamount, Hawaii:
563 Evidence for a relatively dry plume component. Journal of Petrology, 42(3): 627-654.
564 Dixon, J.E., Leist, L., Langmuir, C., Schilling, J.-G., 2002. Recycled dehydrated lithosphere
565 observed in plume-influenced mid-ocean-ridge basalt. Nature, 420(6914): 385-389.
566 Dixon, J.E., Stolper, E.M., 1995. An Experimental Study of Water and Carbon Dioxide
567 Solubilities in Mid-Ocean Ridge Basaltic Liquids. Part II: Applications to Degassing.
568 J. Petrol. 36, 1633-1646.
569 Dixon, J.E., Stolper, E.M., Holloway, J.R., 1995. An experimental study of water and carbon
570 dioxide solubilities in mid ocean ridge basaltic liquids .1. Calibration and solubility
571 models. Journal of Petrology, 36(6): 1607-1631.
572 Farley, K.A., Natland, J.H., Craig, H., 1992. Binary mixing of enriched and undegassed
573 (primitive?) mantle components (He, Sr, Nd, Pb) in Samoan lavas. Earth and
574 Planetary Science Letters, 111(1): 183-199.
575 Fischer, T.P., 2008. Fluxes of volatiles (H2O, CO2, N2, Cl, F) from arc volcanoes. Geochem.
576 J. 42, 21-38.
577 Graham, D.W., 2002. Noble Gas Isotope Geochemistry of Mid-Ocean Ridge and Ocean
578 Island Basalts: Characterisation of Mantle Source Reservoirs. In: Porcelli, D.,

579 Ballentine, C.J., Wieler, R. (Eds.), Noble Gases in Geochemistry and
580 Cosmochemistry. Reviews in Mineralogy and Geochemistry, pp. 245-317.
581 Hahm, D., Hilton, D.R., Castillo, P.R., Hawkins, J.W., Hanan, B.B., Hauri, E.H., 2012. An
582 overview of the volatile systematics of the Lau Basin – Resolving the effects of
583 source variation, magmatic degassing and crustal contamination. Geochimica et
584 Cosmochimica Acta 85, 88-113.
585 Hanyu, T., Tatsumi, Y., Kimura, J.-I., 2011. Constraints on the origin of the HIMU reservoir
586 from He-Ne-Ar isotope systematics. Earth and Planetary Science Letters 307, 377-
587 386.
588 Hauri, E. et al., 2002. SIMS analysis of volatiles in silicate glasses 1. Calibration, matrix
589 effects and comparisons with FTIR. Chemical Geology, 183(1-4): 99-114.
590 Hauri, E.H. et al., 2006. Matrix effects in hydrogen isotope analysis of silicate glasses by
591 SIMS. Chemical Geology, 235(3–4): 352-365.
592 Hekinian, R., Bideau, D., Stoffers, P., Cheminee, J.L., Muhe, R., Puteanus, D., Binard, N.,
593 1991. Submarine intraplate volcanism in the South-Pacific - Geological setting and
594 petrology of the Society and Austral regions. Journal of Geophysical Research-Solid
595 Earth and Planets 96, 2109-2138.
596 Hilton, D.R., Fischer, T.P., Marty, B., 2002. Noble Gases and Volatile Recycling at
597 Subduction Zones, in: Porcelli, D., Ballentine, C., Wieler, R. (Eds.), Noble Gases in
598 Geochemistry and Cosmochemistry. Mineralogical Society of America, Washington
599 D.C., pp. 319-370.
600 Hilton, D.R., Porcelli, D., 2013. Noble Gases as Tracers of Mantle Processes. In: Carlson,
601 R.L. (Ed.), The Mantle and Core - Treatise of Geochemistry. Elsevier, Oxford, pp.
602 277-318.

603 Hofmann, A.W., 2003. Sampling Mantle Heterogeneity through Oceanic Basalts: Isotopes
604 and Trace Elements. In: Carlson, R.L. (Ed.), Treatise of Geochemistry Volume 2: The
605 Core and Mantle. Elsevier Ltd., pp. 61-101.
606 Hofmann, A.W., White, W.M., 1982. Mantle Plumes from Ancient Oceanic-Crust. Earth and
607 Planetary Science Letters, 57(2): 421-436.
608 Holland, G., Ballentine, C.J., 2006. Seawater subduction controls the heavy noble gas
609 composition of the mantle. Nature, 441(7090): 186-191.
610 Honda, M., Woodhead, J.D., 2005. A primordial solar-neon enriched component in the
611 source of EM-I-type ocean island basalts from the Pitcairn Seamounts, Polynesia.
612 Earth and Planetary Science Letters, 236(3-4): 597-612.
613 Iacono-Marziano, G., Morizet, Y., Le Trong, E., Gaillard, F., 2012. New experimental data
614 and semi-empirical parameterization of H2O-CO2 solubility in mafic melts.
615 Geochimica et Cosmochimica Acta 97, 1-23.
616 Ito, E., Harris, D.M., Anderson, A.T., 1983. Alteration of Oceanic-Crust and Geologic
617 Cycling of Chlorine and Water. Geochimica et Cosmochimica Acta, 47(9): 1613-
618 1624.
619 Jackson, C.R.M., Parman, S.W., Kelley, S.P., Cooper, R.F., 2013. Noble gas transport into
620 the mantle facilitated by high solubility in amphibole. Nature Geosci, 6(7): 562-565.
621 Jackson, M.G., Carlson, R.W., Kurz, M.D., Kempton, P.D., Francis, D., Blusztajn, J., 2010.
622 Evidence for the survival of the oldest terrestrial mantle reservoir. Nature 466, 853-
623 856.
624 Jackson, M.G., Hart, S.R., Koppers, A.A.P., Staudigel, H., Konter, J., Blusztajn, J., Kurz, M.,
625 Russell, J.A., 2007. The return of subducted continental crust in Samoan lavas. Nature
626 448, 684-687.

627 Jacobsen, S.D., van der Lee, S., 2006. Earth's Deep Water Cycle. Geophys. Monogr. Ser.,
628 168. AGU, Washington, DC, 313 pp.
629 Jambon, A., Deruelle, B., Dreibus, G., Pineau, F., 1995. Chlorine and bromine abundance in
630 MORB: The contrasting behaviour of the Mid-Atlantic Ridge and East Pacific Rise
631 and implications for chlorine geodynamic cycle. Chemical Geology 126, 101-117.
632 Jambon, A., Zimmermann, J.L., 1990. Water in oceanic basalts - evidence for dehydration of
633 recycled crust. Earth and Planetary Science Letters 101, 323-331.
634 John, T., Layne, G.D., Haase, K.M., Barnes, J.D., 2010. Chlorine isotope evidence for crustal
635 recycling into the Earth's mantle. Earth and Planetary Science Letters 298, 175-182.
636 John, T., Scambelluri, M., Frische, M., Barnes, J.D., Bach, W., 2011. Dehydration of
637 subducting serpentinite: Implications for halogen mobility in subduction zones and
638 the deep halogen cycle. Earth and Planetary Science Letters, 308(1-2): 65-76.
639 Kendrick, M.A., 2012. High precision Cl, Br and I determination in mineral standards using
640 the noble gas method. Chemical Geology 292-293, 116-126.
641 Kendrick, M.A., Arculus, R.J., Burnard, P., Honda, M., 2013a. Quantifying brine assimilation
642 by submarine magmas: Examples from the Galápagos Spreading Centre and Lau
643 Basin. Geochimica et Cosmochimica Acta 123, 150-165.
644 Kendrick, M.A., Honda, M., Pettke, T., Scambelluri, M., Phillips, D., Giuliani, A., 2013b.
645 Subduction zone fluxes of halogens and noble gases in seafloor and forearc
646 serpentinites. Earth and Planetary Science Letters 365, 86-96.
647 Kendrick, M.A., Kamenetsky, V.S., Phillips, D., Honda, M., 2012a. Halogen (Cl, Br, I)
648 systematics of mid-ocean ridge basalts: a Macquarie Island case study. Geochimica et
649 Cosmochimica Acta, 81: 82-93.

650 Kendrick, M.A., Scambelluri, M., Honda, M., Phillips, D., 2011. High abundances of noble
651 gas and chlorine delivered to the mantle by serpentinite subduction. Nature
652 Geoscience, 4: 807-812.
653 Kendrick, M.A., Woodhead, J.D., Kamenetsky, V.S., 2012b. Tracking halogens through the
654 subduction cycle. Geology, 40(12): 1075-1078.
655 Kent, A.J.R. et al., 1999a. Widespread assimilation of a seawater-derived component at Loihi
656 Seamount, Hawaii. Geochimica et Cosmochimica Acta, 63(18): 2749-2761.
657 Kent, A.J.R., Norman, M.D., Hutcheon, I.D., Stolper, E.M., 1999b. Assimilation of seawater-
658 derived components in an oceanic volcano: evidence from matrix glasses and glass
659 inclusions from Loihi seamount, Hawaii. Chemical Geology, 156(1-4): 299-319.
660 Kent, A.J.R., Peate, D.W., Newman, S., Stolper, E.M., Pearce, J.A., 2002. Chlorine in
661 submarine glasses from the Lau Basin: seawater contamination and constraints on the
662 composition of slab-derived fluids. Earth and Planetary Science Letters, 202(2): 361-
663 377.
664 Kent, A.J.R., Stolper, E.M., Francis, D., Woodhead, J., Frei, R., Eiler, J., 2004. Mantle
665 heterogeneity during the formation of the North Atlantic Igneous Province:
666 Constraints from trace element and Sr-Nd-Os-O isotope systematics of Baffin Island
667 picrites. Geochemistry, Geophysics, Geosystems 5, Q11004.
668 King PL, Vennemann TW, Holloway JR, Hervig RL, Lowenstern JB, Forneris JF (2002)
669 Analytical techniques for volatiles: A case study using intermediate (andesitic)
670 glasses. Amer Mineral 87:1077-1089
671 Kohlstedt, D.L., Keppler, H., Rubie, D.C., 1996. Solubility of water in the alpha, beta and
672 gamma phases of (Mg,Fe)(2)SiO4. Contributions to Mineralogy and Petrology,
673 123(4): 345-357.

674 Kurz, M.D., Jenkins, W.J., Hart, S.R., 1982. Helium isotopic systematics of oceanic islands
675 and mantle heterogeneity. Nature, 297: 43-46.
676 Le Bas, M.J., Streckeisen, A.L., 1991. The IUGS systematics of igneous rocks. Journal of the
677 Geological Society, London 148, 825-833.
678 le Roux, P.J., Shirey, S.B., Hauri, E.H., Perfit, M.R., Bender, J.F., 2006. The effects of
679 variable sources, processes and contaminants on the composition of northern EPR
680 MORB (8-10 degrees N and 12-14 degrees N): Evidence from volatiles (H2O, CO2,
681 S) and halogens (F, Cl). Earth and Planetary Science Letters, 251(3-4): 209-231.
682 Mandeville CW, Webster JD, Rutherford MJ, Taylor BE, Timbal A, Faure K (2002)
683 Determination of molar absorptivities in infrared absorption bands of H2O in
684 andesitic glasses. Amer. Mineral 87:813-821
685 Michael, P., 1995. Regionally distinctive sources of depleted MORB - evidence from trace
686 elements and H2O. Earth and Planetary Science Letters 131, 301-320.
687 Michael, P.J., Cornell, W.C., 1998. Influence of spreading rate and magma supply on
688 crystallization and assimilation beneath mid-ocean ridges: Evidence from chlorine
689 and major element chemistry of mid-ocean ridge basalts. J. Geophys. Res.-Solid Earth
690 103, 18325-18356.
691 Schilling, J.C., Unni, C.K., Bender, M.L., 1978. Origin of Chlorine and Bromine in the
692 oceans. Nature 273, 631-636.crystallization and assimilation beneath mid-ocean
693 ridges: Evidence from chlorine and major element chemistry of mid-ocean ridge
694 basalts. Journal of Geophysical Research-Solid Earth, 103(B8): 18325-18356.
695 Mukhopadhyay, S., 2012. Early differentiation and volatile accretion recorded in deep-mantle
696 neon and xenon. Nature, 486(7401): 101-104.
697 Newman, S., Lowenstern, J.B., 2002. VOLATILECALC: a silicate melt-H2O-CO2 solution
698 model written in Visual Basic for excel. Computers & Geosciences, 28(5): 597-604.

699 Parai, R., Mukhopadhyay, S., Lassiter, J.C., 2009. New constraints on the HIMU mantle from
700 neon and helium isotopic compositions of basalts from the Cook-Austral Islands.
701 Earth and Planetary Science Letters 277, 253-261
702 Parai, R., Mukhopadhyay, S., 2012. How large is the subducted water flux? New constraints
703 on mantle regassing rates. Earth and Planetary Science Letters, 317: 396-406.
704 Philippot, P., Agrinier, P., Scambelluri, M., 1998. Chlorine cycling during subduction of
705 altered oceanic crust. Earth and Planetary Science Letters 161, 33-44.
706 Plank, T., Langmuir, C.H., 1998. The chemical composition of subducting sediment and its
707 consequences for the crust and mantle. Chemical Geology, 145(3-4): 325-394.
708 Portnyagin, M., Hoernle, K., Plechov, P., Mironov, N., Khubunaya, S., 2007. Constraints on
709 mantle melting and composition and nature of slab components in volcanic arcs from
710 volatiles (H2O, S, Cl, F) and trace elements in melt inclusions from the Kamchatka
711 Arc. Earth and Planetary Science Letters, 255(1–2): 53-69.
712 Rowe, M.C., Kent, A.J.R., Nielsen, R.L., 2009. Across Arc Variation in Basaltic fO2:
713 Influence of a Subduction Component in the Cascadia Subduction Zone. Journal of
714 Petrology, 50: 61-91.
715 Rüpke, L.H., Morgan, J.P., Hort, M., Connolly, J.A.D., 2004. Serpentine and the subduction
716 zone water cycle. Earth and Planetary Science Letters, 223(1-2): 17-34.
717 Schilling, J.C., Unni, C.K., Bender, M.L., 1978. Origin of Chlorine and Bromine in the
718 oceans. Nature 273, 631-636.
719 Schilling, J.G., Bergeron, M.B., Evans, R., 1980. Halogens in the mantle beneath the North
720 Atlantic. Philosophical Transactions of the Royal Society of London Series a-
721 Mathematical Physical and Engineering Sciences, 297(1431): 147-178.

722 Shaw, A.M., Hauri, E.H., Behn, M.D., Hilton, D.R., Macpherson, C.G., Sinton, J.M., 2012.
723 Long-term preservation of slab signatures in the mantle inferred from hydrogen
724 isotopes. Nat. Geosci. 5, 224-228.
725 Sinton, J., Ford, L.L., Chappell, B., McCulloch, M.T., 2003. Magma Genesis and Mantle
726 Heterogeneity in the Manus Back-Arc Basin, Papua New Guinea. Journal of
727 Petrology, 44: 159-195.
728 Smyth, J.R., Frost, D.J., Nestola, F., Holl, C.M., Bromiley, G., 2006. Olivine hydration in the
729 deep upper mantle: Effects of temperature and silica activity. Geophysical Research
730 Letters 33
731 Staudacher, T., Allègre, C.J., 1988. Recycling of oceanic crust and sediments: the noble gas
732 subduction barrier. Earth and Planetary Science Letters 89, 173-183.
733 Staudacher, T., Allègre, C.J., 1989. Noble gases in glass samples from Tahiti: Teahitia,
734 Rocard and Mehetia. Earth and Planetary Science Letters 93, 210-222.
735 Stoffers, P., 1987. Cruise report SONNE 47 - Midplate volcanism central South Pacific,
736 French Polynesia. Tahiti-Tahiti, 27-12-1986 - 2-2-1987. Ber. Rep. Geol. Inst. Kiel.
737 Univ, 19: 180.
738 Stoffers, P., Hekinian, R., Ackermand, D., Binard, N., Botz, R., Devey, C., Hansen, D.,
739 Hodkinson, R., Jeschke, G., Lange, J., Perre, E.v., Scholten, J., Schmitt, M., Sedwick,
740 P., Woodhead, J.D., 1990. Active Pitcairn Hotspot Found. Marine Geology 95, 51-55.
741 Stracke, A., 2012. Earth's heterogeneous mantle: A product of convection-driven interaction
742 between crust and mantle. Chemical Geology 330, 274-299.
743 Straub, S.M., Layne, G.D., 2003. The systematics of chlorine, fluorine, and water in Izu arc
744 front volcanic rocks: Implications for volatile recycling in subduction zones.
745 Geochimica Et Cosmochimica Acta, 67(21): 4179-4203.

746 Stroncik, N.A., Haase, K.M., 2004. Chlorine in oceanic intraplate basalts: Constraints on
747 mantle sources and recycling processes. Geology, 32(11): 945-948.
748 Unni, C.K., Schilling, J.G., 1978. Cl and Br Degassing by Volcanism Along Reykjanes Ridge
749 and Iceland. Nature, 272(5648): 19-23.
750 Vigouroux, N., Wallace, P.J., Williams-Jones, G., Kelley, K., Kent, A.J.R., Williams-Jones,
751 A.E., 2012. The sources of volatile and fluid-mobile elements in the Sunda arc: A
752 melt inclusion study from Kawah Ijen and Tambora volcanoes, Indonesia. Geochem.
753 Geophys. Geosyst. 13.
754 Wallace, P.J., 2002, Volatiles in Submarine basaltic glasses from the Northern Kerguelen
755 Plateau (ODP Site 1140): Implications from source region compositions, magmatic
756 processes, and plateau subsidence, Journal of Petrology 43, 1311-1326.
757 Wallace, P.J., 2005. Volatiles in subduction zone magmas: concentrations and fluxes based
758 on melt inclusion and volcanic gas data. Journal of Volcanology and Geothermal
759 Research, 140(1-3): 217-240.
760 Wanless, V.D., Perfit, M.R., Ridley, W.I., Wallace, P.J., Grimes, C.B., Klein, E.M., 2011.
761 Volatile abundances and oxygen isotopes in basaltic to dacitic lavas on mid-ocean
762 ridges: The role of assimilation at spreading centers. Chemical Geology 287, 54-65.
763 Webster, J.D., Kinzler, R.J., Mathez, E.A., 1999. Chloride and water solubility in basalt and
764 andesite melts and implications for magmatic degassing. Geochimica Et
765 Cosmochimica Acta 63, 729-738.
766 White, W.M., 2010, Oceanic Island Basalts and Mantle Plumes: The Geochemical
767 Perspective: Annual Review of Earth and Planetary Sciences, v. 38, no. 1, p. 133-160,
768 doi: 10.1146/annurev-earth-040809-152450.

769 Workman, R.K., Hauri, E., Hart, S.R., Wang, J., Blusztajn, J., 2006. Volatile and trace
770 elements in basaltic glasses from Samoa: Implications for water distribution in the
771 mantle. Earth and Planetary Science Letters 241, 932-951.

772 Woodhead, J.D., Devey, C.W., 1993. Geochemistry of the Pitcairn Seamounts. 1. Source
773 Character and Temperal Trends. Earth and Planetary Science Letters, 116(1-4): 81-99.

774 Zindler, A., and Hart, S., 1986, Chemical geodynamics: Annual Review of Earth and
775 Planetary Sciences, v. 14, p. 493-571.

Table 1. Sample information and volatile content of Pitcairn glasses

Sample	**SO65 45DS-1**	**SO65 46DS -2**	**SO65 46DS -7**	**SO65 48DS-6**	**SO65 49DS-1**	**SO65 51DS-1**	**SO65 51DS-2**	**SO65 51DS-4**	**SO65 51DS-9**	**SO65 52DS-1**	**SO65 33GTV2**	**SO65 57DS-1**	**SO65 57DS-6**	**SO65 57DS-8**
Volcano	**Volc. 2**	**Volc. 2**	**Volc. 2**	**Volc. 2**	**Volc. 2**	**Volc. 2**	**Volc. 2**	**Volc. 2**	**Volc. 2**	**Volc. 2**	**Volc. 2**	**Volc. 5**	**Volc. 5**	**Volc. 5**
Dredge depth (m)	490-610	760-770	760-770	1290-1420	1970-2080	1610-1860	1610-1860	1610-1860	1610-1860	2800-2850	410	2500-2820	2500-2820	2500-2820
Eqm. P –V.Calc (bar)	57	82	82	190	210	180		210	180	340		310	310	
Eqm. P – Alt. (bar)	140	190	120	220	210	190		380	190	600		480	490	
Volatile content														
H_2O wt % (SIMS)	0.75	0.83	0.84	1.1	0.83	0.76		1.4	0.79	1.6		1.5	1.5	
H_2O wt % (FTIR)	0.81	0.85	0.84	1.1	1.0	0.80		1.6	0.78	1.8		1.5	1.6	
CO_2 ppm (SIMS)	2.3	7.8	7.1	31	68	58		5.6	55	39		38	39	
S ppm (SIMS)	300	760	770	1240	790	1150		490	1160	510		690	700	
S ppm (EPMA)	260	770	780	1220	810	1150	1400	670	1130	430	510	610	620	650
F ppm (SIMS)	1460	790	800	840	670	480		1160	490	1790		1440	1440	
Cl ppm (SIMS)	910	550	560	470	380	250		890	250	650		540	540	
Cl ppm (EPMA)	930	580	630	530	450	390	280	1000	280	670	680	610	580	560
Cl ppm (NG)*	860	630		500	420		280	860	270	670	660			550
Br ppb (NG)*	3000	2100		1700	1300		870	2500	840	2100	2100			1900
I ppb (NG)*	53	33		38	27		22	58	21	51	37			53
Selected major elements (wt. %)														
MgO	2.9	5.3	5.3	4.7	5.7	5.8	5.6	2.6	5.9	2.1	4.8	2.8	2.8	2.7
SiO_2	55.6	49.5	49.1	49.2	49.1	50.5	50.4	54.9	51.1	55.3	48.9	55.7	54.8	54.8
Selected trace elements (ppm)														
Ce	174	88	88	92	95	54	71	118	53	193	144	192	184	227
Nb	78	45	45	47	46	26	33	56	25	92	586	75	72	84
Dy	9.7	7.2	7.1	7.3	6.1	5.3	8.1	10	6.0	12	11	14	12	16
Cu	21	48	50	52	62	49		11	49	1.6		5.8	5.7	
Nd	79	48	46	48	45	30	43	64	31	91	78	98	93	117
K	25,500	12,400	12,200	14,000	13,700	7600	*7,500*	17,800	7200	28,900	*14,700*	20,400	21,100	*23,700*
Sm	15	11	10	10	9.0	7.0	10	14	7.4	17	17	20	19	24
La	76	39	39	44	44	22	32	53	24	95	66	90	87	108
$(La/Sm)_N$	3.2	2.3	2.4	2.7	3.1	2.0	2.0	2.4	2.0	3.5	2.4	2.8	2.9	2.9
Selected isotopes*														
$^{87}Sr/^{86}Sr$	0.70492	0.70423	0.70427	0.70425	0.70501	0.70443	0.70443	0.70393	0.70443	0.70519	0.70410	0.70527	0.70530	0.70528
$^{144}Nd/^{143}Nd$	0.51253	0.51269	0.51272	0.51263	0.51250	0.51266	0.51266	0.51281	0.51270	0.51248	0.51271	0.51248	0.51248	0.51246
$^{206}Pb/^{204}Pb$	17.74	18.04	18.04	17.85	17.62	17.95	17.94	18.19	17.95	17.45	18.12	17.51	17.51	17.51
$^{3}He/^{4}He$ (R/Ra)	9.1	(9.1)	9.9	7.7	9.3	7.9	7.6	(3.6)	10.6	(1.6)		(4.4)		(6.9)

** Revised Br and I concentrations from Kendrick et al. (2012b). Isotope data from Woodhead and Devey (1993); Honda and Woodhead (2005). Note that samples containing ^{4}He of $<10^{-7}$ cm^3 STP/g (in brackets), include all samples with $^{3}He/^{4}He$ ratios of <7 R/Ra (Ra = the atmospheric $^{3}He/^{4}He$ ratio of 1.39×10^{-6}), are not considered representative of the parental magma (Honda and Woodhead, 2005). Note equilibrium degassing pressures have been calculated for basaltic melts containing 49 wt % SiO_2 using VolatileCalc (V.Calc.) and an alternative (Alt.) solubility model (Iacono-Marziano et al., 2012).*

Table 2. Sample information and volatile content of Society glasses

Cruise/Sample	CH-DR1 P1-1	CH-DR1 P3-4	CH-DR4 4-2	CH-DR4 4-3	CH-DR4 4-1	CH-DR3 3-1	SO47 9DS-1	CH-DR2 2-1	SO47 29DS-1	SO47 81DS-3
Volcano	Mehetia	Mehetia	Rocard	Rocard	Rocard	Teahitia	Teahitia	NW of Teahitia	Moua Pihaa	Cyana
Dredge depth (m)	2500-2700*2	2500-2700	2500-3000*2	2500-3000*2	2500-3000*2	2100-2600	2360-2800	3000-3500	2200-2660	2100-2600
Eqm. P –V.Calc (bar)		310	220*	250*		190	370		370	180*
Eqm. P – Alt. (bar)		310				220	330		380	
Volatile content										
H_2O wt % (SIMS)		1.5	1.3	1.3		0.91	0.95		1.4	1.1
H_2O wt % (FTIR)		1.6	1.5	1.6		0.84	0.95		1.5	1.4
CO_2 ppm (SIMS)		75	19	32		100	160		160	17
S ppm (SIMS)		2490	250	280		1020	980		1800	430
S ppm (EPMA)		2200	220	240	190	1030	980	1300	1610	390
F ppm (SIMS)		1450	2010	2090		1050	1100		1860	990
Cl ppm (SIMS)		950	1350	1360		920	580		1410	1240
Cl ppm (EPMA)		1010	1410	1320	1280	1000	630	940	1460	1300
Cl ppm (NG)*	610	1000	1450	1380	1340	960	590	1030	1180	1210
Br ppb (NG)*	1900	2800	3700	3500	3600	3700	1700	2900	3500	3600
I ppb (NG)*	28	46	71	67	70	42	38	77	49	59
Selected major elements (wt. %)										
MgO		5.3	1.4	1.5	1.2	6.9	6.0	6.4	5.2	1.07
SiO_2		44.9	61.3	60.9	59.8	45.9	48.6	44.3	44.9	65.2
Selected trace elements (ppm)										
Ce		121	247	216	342	94	110	161	139	141
Nb		66	176	154	220	44	50	75	84	89
Dy		6.9	11	9.1	16	5.7	6.8	10	8.4	6.2
Cu		53	0.5	0.4		94	68		15	0.3
Nd		61	149	104	90	50	59	85	69	60
K		16,200	48,300	50,100	*48,400*	14,100	20,100	*17,200*	17,900	46,400
Sm		13	18	16	27	10	12	18	14	11
La		53	112	98	162	39	50	74	61	64
$(La/Sm)_N$	2.7	2.6	3.8	3.8	3.7	2.4	2.6	2.6	2.7	3.8
Selected isotopes*										
$^{87}Sr/^{86}Sr$	0.70466	0.70428	0.70593	0.70587		0.70464	0.70551		0.70371	0.70450
$^{144}Nd/^{143}Nd$	0.51276	0.51289	0.51258	0.51265		0.51271	0.51271		0.51293	0.51289
$^{206}Pb/^{204}Pb$	19.10	19.10	19.21	19.22		19.13	19.12	19.10	19.22	18.99
$^{3}He/^{4}He$ (R/Ra)		11.1	7.4		7.8					

** Revised Br and I concentrations from Kendrick et al. (2012b). Isotope data from Devey et al. (1990); Staudacher and Allegre (1989), 3He/4He data are reported relative to the Ra, the atmospheric $^{3}He/^{4}He$ ratio of 1.39×10^{-6}. *2 'popping rocks' (Hekinian et al., 1991). Note equilibrium degassing pressures calculated with VolatileCalc (V.Calc.) assumed basaltic composition with <49 wt % SiO_2 and a rhyolite* compositions for melts with >60 wt % SiO_2. An alternative (Alt.) pressure was calculated for the least evolved melts using the solubility model of Iacono-Marziano et al. (2012).*

Table 3. Matrix and vesicle volatile contents

Sample	Matrix (SIMS)		Vesicles (crushing)[1]			% in Vesicles	
	CO_2 ppm	H_2O Wt %	Vol. %	CO_2 ppm	H_2O Wt %	CO_2	H_2O
CH DR1 P3-4	75	1.5	29%	2831	0.41	97%	21%
CH DR4 4-2	19	1.3	8.6%	372	0.15	95%	10%

1 – Data of Aubaud et al. (2005).

Table 4. Representative magma volatile characteristics in different settings[1]

	H_2O/Ce	**H_2O/Cl**	**F/Cl**	**Br/Cl $\times10^{-3}$**	**I/Cl $\times10^{-5}$**	**K/Cl**
Mantle-derived melts						
Arc/Back Arc Basin Basalts[2]	1000-3000	5-80	0.2-1.5	1-3.2	3-90	~1
MORB[3]	150-250	10-50	~1-10	2.8-3.2	3-9	10-20
EM1 Pitcairn	80	30-40	1.5-3	2.8	5-9	>40
EM2 Society/Samoa	60	10-20	1.5-3	3.2	4-8	>40

1 – The data are compiled from published analyses of melt inclusions or submarine glasses that have not been affected by degassing or assimilation of seawater-derived components [which would reduce all X/Cl ratios (except Br/Cl) to lower values (Kendrick et al., 2013a)].
2- Manus Basin (Sinton et al., 2003; Kendrick et al., 2012b;Shaw et al., 2012); Kamchatka Arc (Portnyagin et al., 2007); Izu-Bonnin Arc (Straub and Layne, 2003); Sunda Arc (Vigouroux et al, 2012); Lau Basin (Hahm et al., 2012).
3 - Jambon et al. (1995); Kendrick et al. (2012a; 2013a); Micheal (1995); Schilling et al. (1978; 1980).

Fig 1

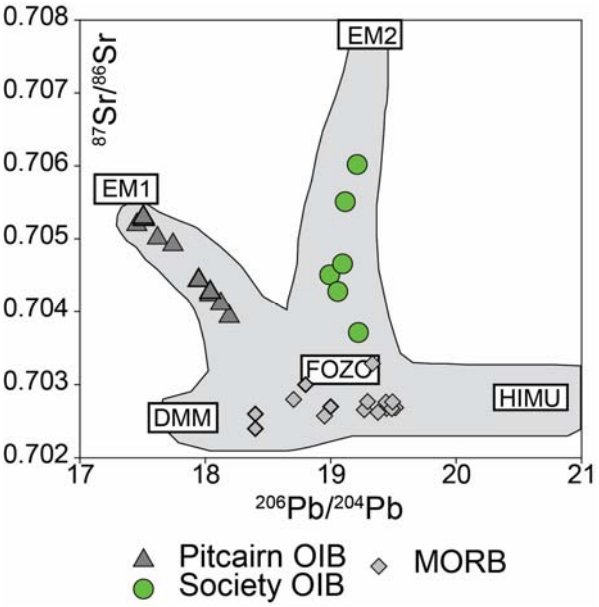

Fig 1. The $^{206}Pb/^{204}Pb$ versus $^{87}Sr/^{86}Sr$ systematics of the Pitcairn and Society melts included this study (Devey et al., 1990; Honda and Woodhead, 2005). MORB from two previous halogen studies are shown for reference (Kendrick et al., 2013a; 2012a), note that MORB occupy a large part of this diagram with typical $^{87}Sr/^{86}Sr$ in the range of 0.7021-0.7035 and $^{206}Pb/^{204}Pb$ in the range of 17.5 to 19.5 (see Hofmann, 2003 or Stracke, 2012).

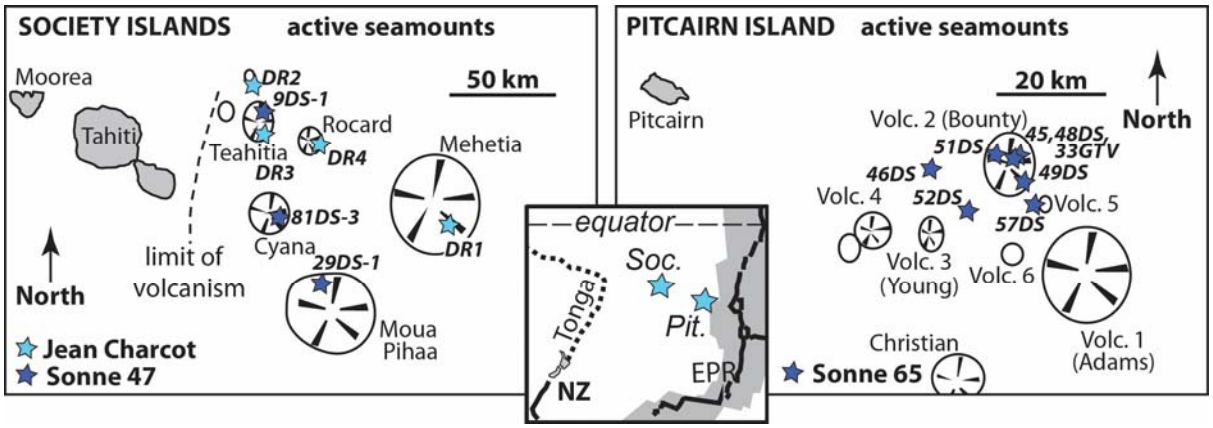

Fig 2. Sketch locality maps showing the approximate positions of dredges undertaken during voyages of the FS Sonne and NO Jean Charcot to the Society and Pitcairn seamounts during the 1980's. Bathymetric data and dredge locations for these localities were reported in Cheminee et al. (1989), Stoffers et al. (1987; 1990) and Devey et al. (1990; 2003). The inset shows the positions of the Society and Pitcairn seamount chains in the South Pacific, with respect to the East Pacific Rise (EPR), Tonga Trench and New Zealand (NZ).

Fig 3

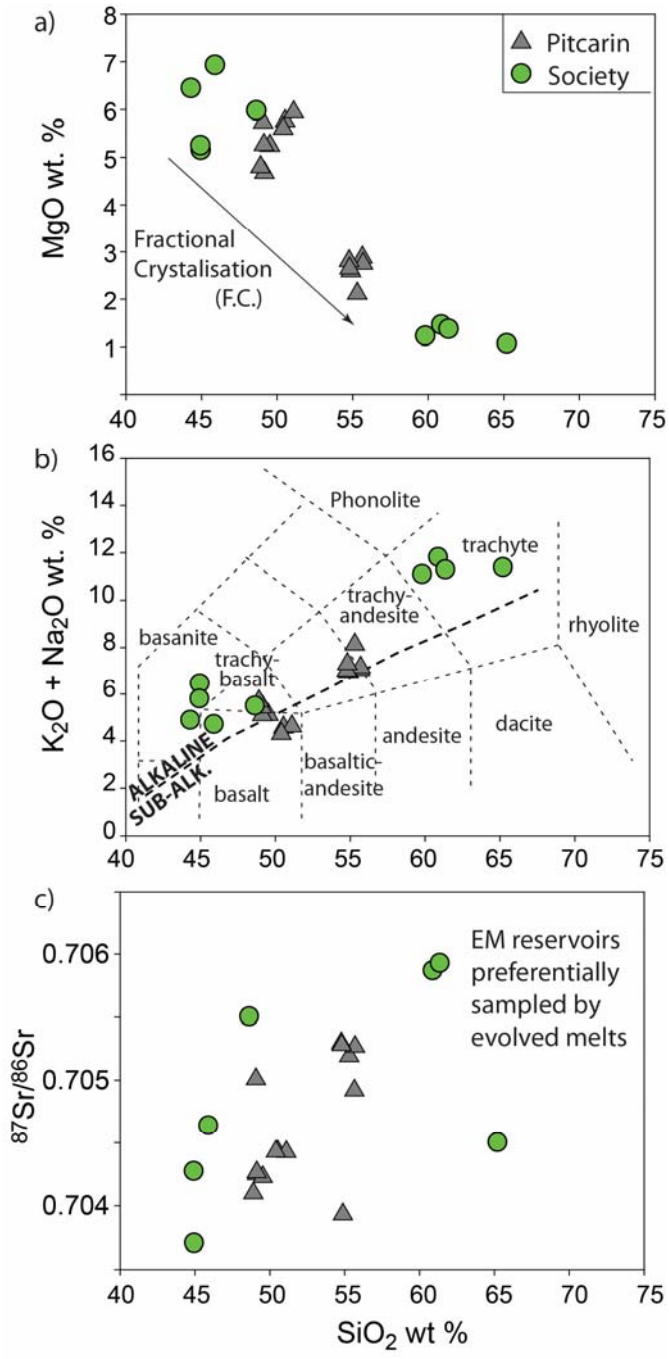

Fig 3. ab) Major element compositions of Pitcairn and Society glasses with classification after Le Bas and Streckeisen (1986). c) SiO_2 versus $^{87}Sr/^{86}Sr$.

Fig 4

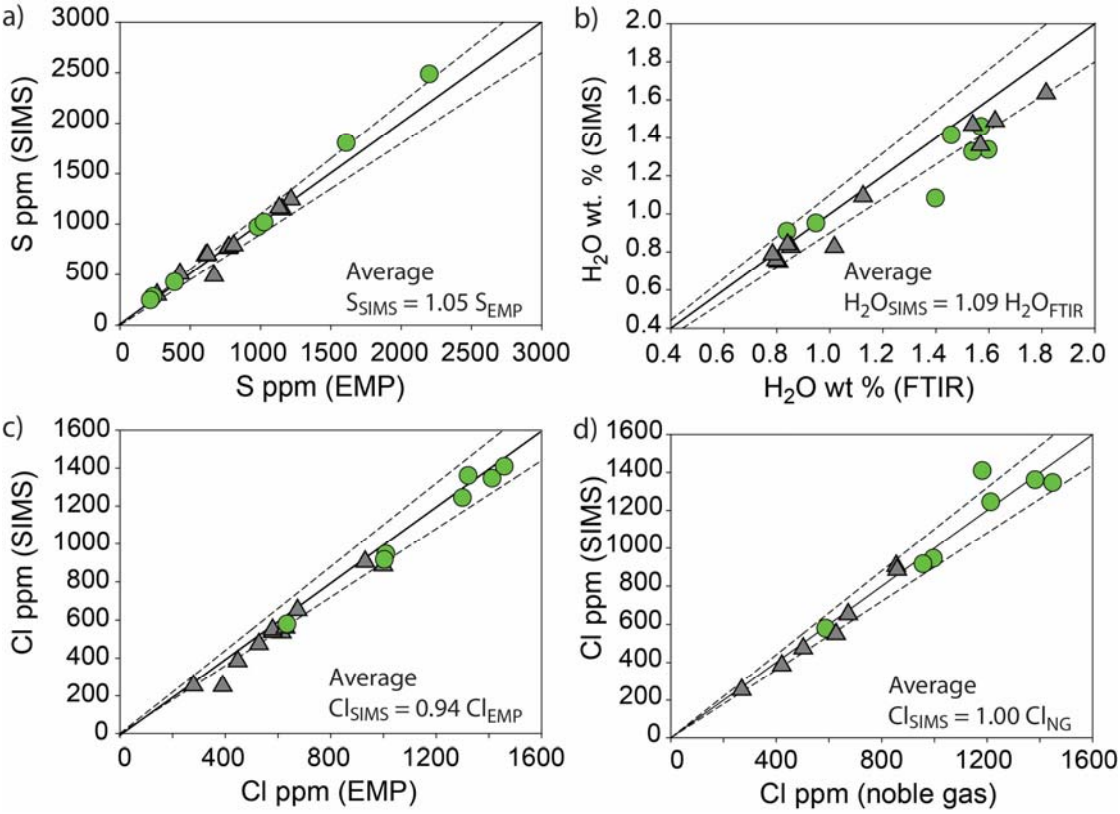

Fig 4. Comparison of S, H_2O and Cl measurements by electron microprobe at Oregon State University, FTIR at the University of Oregon, SIMS at the Carnegie Institute and the noble gas method at the University of Melbourne. The 1:1 line and 10% envelopes are shown in each plot together with the average difference between the techniques which is based on best fit data regressions forced through the origin.

Fig 5

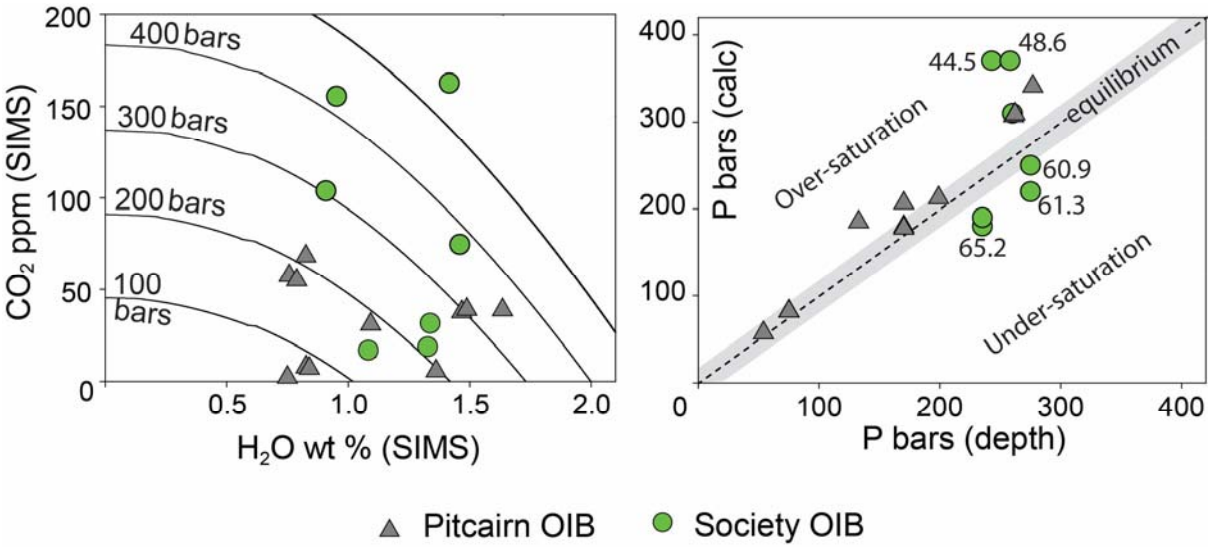

Fig 5. a) SIMS CO_2 and H_2O concentrations in Society and Pitcairn melts showing isobars (lines of constant pressure) calculated for a basalt with 49 wt % SiO_2 at 1200 °C using the VolatileCalc program (Newman and Lowenstern, 2002). b) Pressure in bars estimated from the dredging depth and calculated for the H_2O and CO_2 concentrations using VolatileCalc (Table 1 and 2; note that Society samples with >60 wt % SiO_2 were modelled as rhyolite).

Fig 6

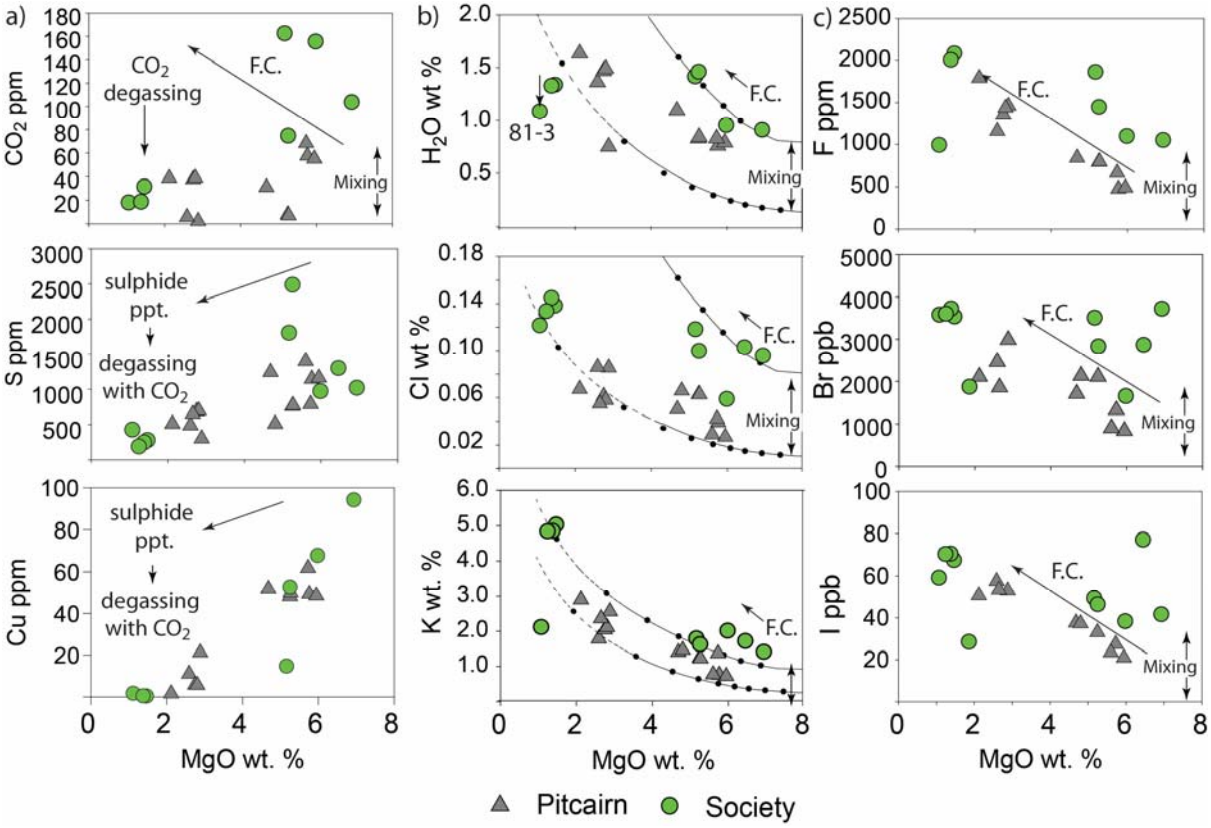

Fig 6. Pitcairn and Society glass volatile and incompatible element concentrations as a function of MgO. Column a) CO_2, S and Cu (a chalcophile element); column b) H_2O, Cl and K (a lithophile element with incompatibility similar to Cl and H_2O). Liquid lines of descent calculated with Petrolog3 (Danyushevsky and Plechov, 2011) are shown for fractional crystallisation of hypothetical MORB and enriched-mantle (OIB) components assuming H_2O, Cl and K are excluded from all crystallising phases (see text). Increments of 10% are shown, with melts of ~1 wt % MgO produced by crystallisation of ~80-85% of the original magma. column c) F, Br and I concentrations are governed by similar processes as Cl, but modelled liquid lines of descent are not shown.

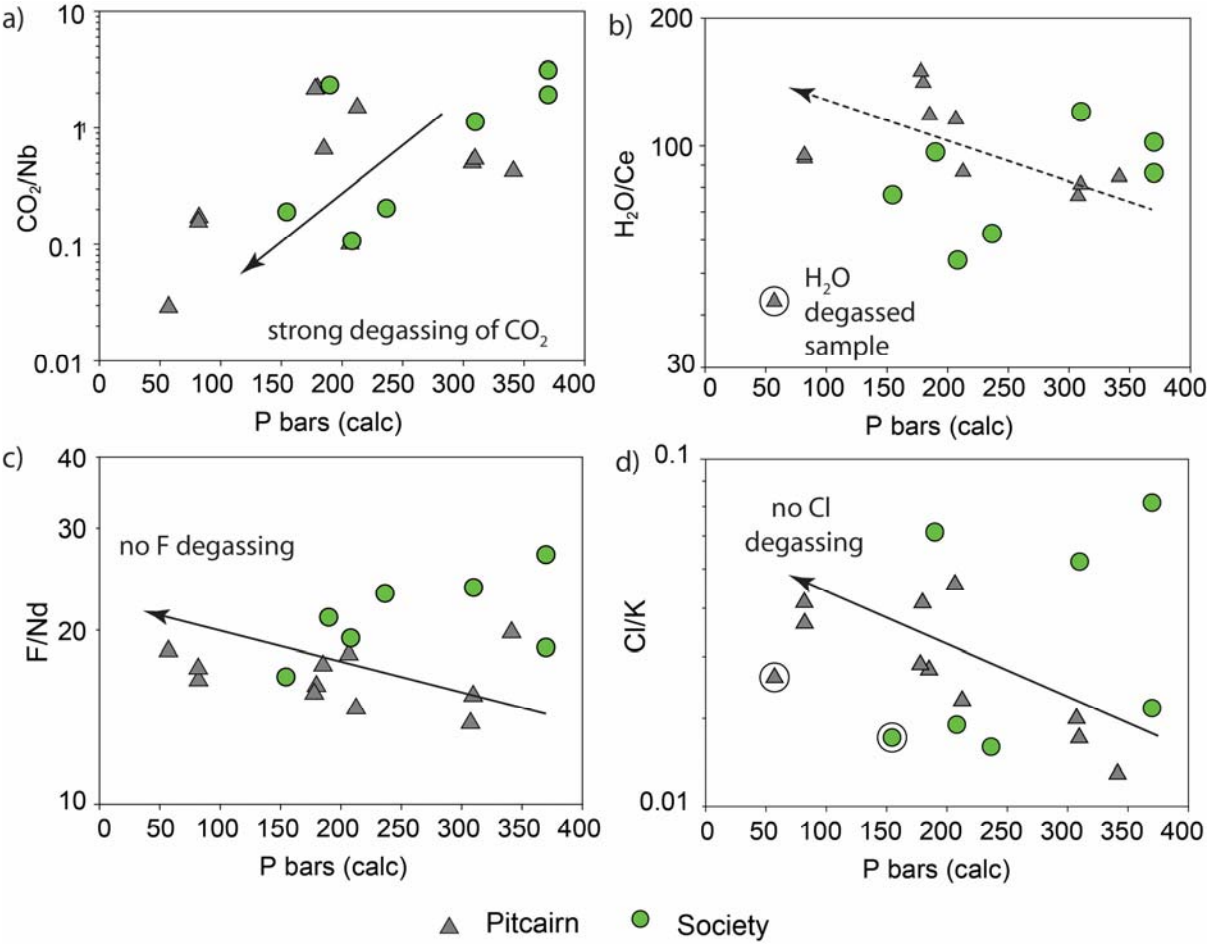

Fig 7. Volatile/non-volatile ratios of CO_2/Nb, H_2O/Ce, Cl/K and F/Nd as a function of calculated equilibration depth (see Fig 5b). Melts equilibrated at pressures of more than 150 bars are suggested to have retained their H_2O as well as halogens during degassing.

Fig 8

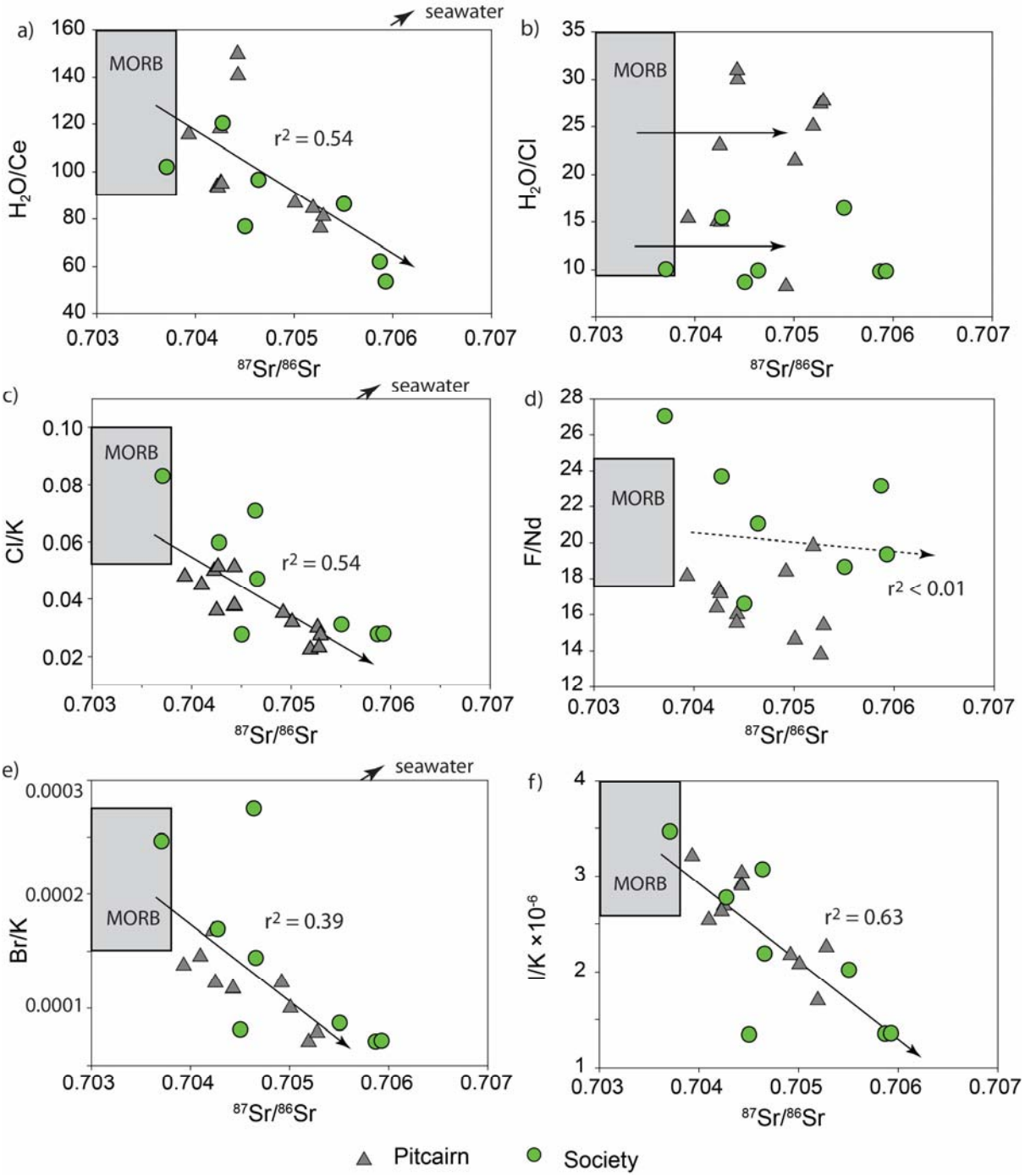

Fig 8 Volatile/non-volatile ratios of H_2O/Ce, Cl/K, F/Nd, Br/K and I/K and the H_2O/Cl ratio as a function of mantle enrichment measured by $^{87}Sr/^{86}Sr$. Note that for clarity, the H_2O data are not shown for 45-DS-1 which is indicated to have lost H_2O in Fig 7b. The correlation coefficients in each plot are for the slopes defined by the combined Pitcairn and Society data.

Fig 9

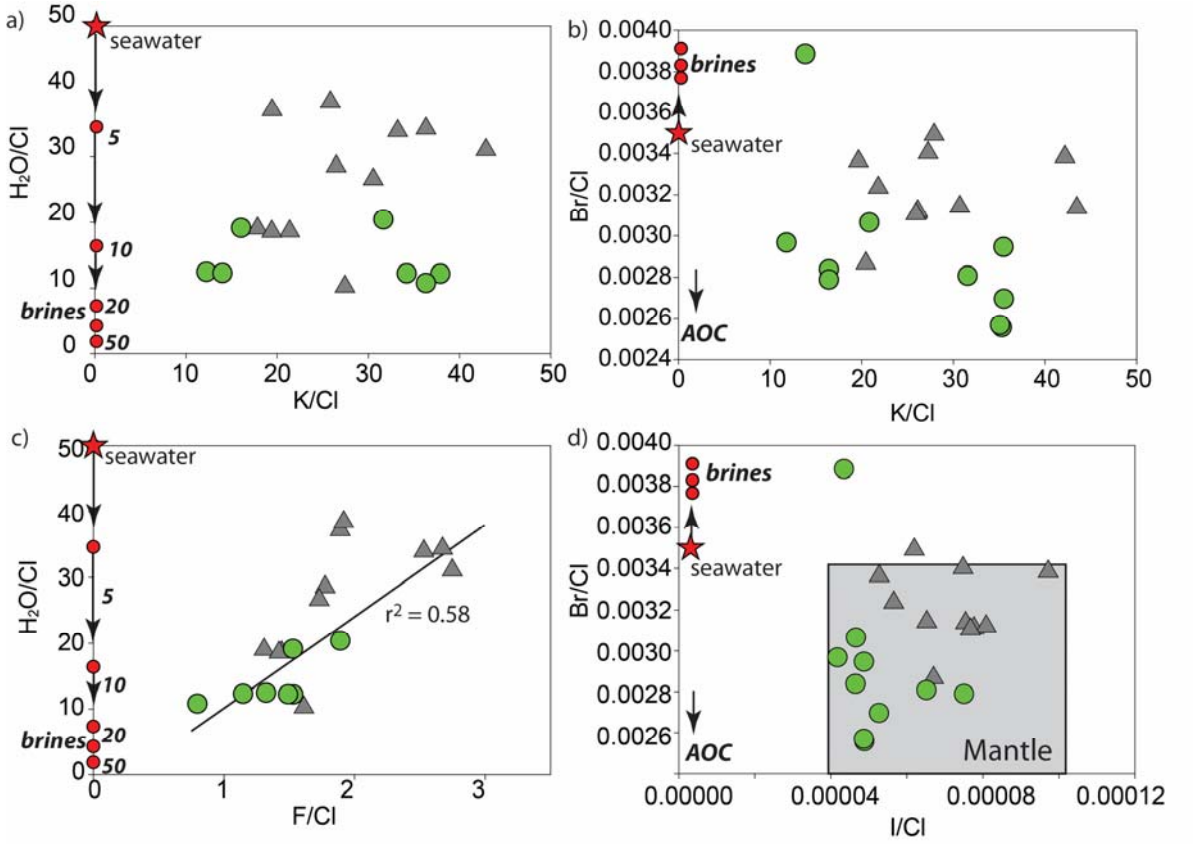

Fig 9. Halogen and H_2O data for the Pitcairn and Society melts. Assimilation of seawater-components such as high salinity brines would produce strong co-variation in Br/Cl, I/Cl, F/Cl, K/Cl and H_2O/Cl which is not observed. High salinity brines are characterised by higher than seawater Br/Cl ratios, whereas altered ocean crust (AOC) is expected to have lower than seawater Br/Cl (Kendrick et al., 2013a). The italicised bold numbers inside the H_2O/Cl axes indicate salinity in wt % salts. Note that the mantle field in d is based on the compiled data of Kendrick et al. (2013a) which show no significant difference between OIB and MORB (see also Schilling et al 1978; 1980).

Fig 10

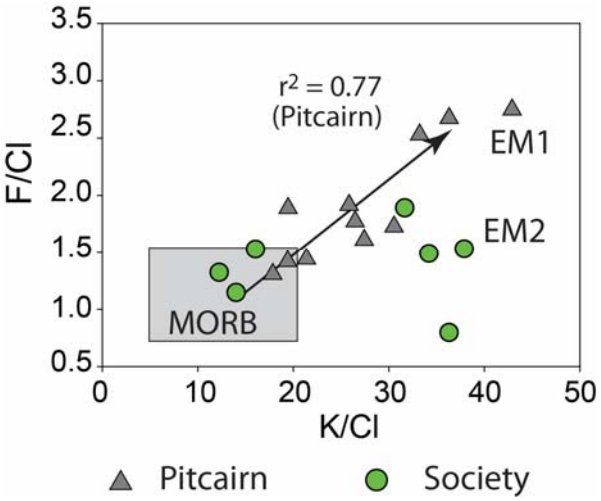

Fig 10. F/Cl versus K/Cl in Pitcairn and Society melts. K/Cl increases toward the enriched mantle end-member because K is preferentially subducted into the mantle compared to Cl (Fig 9c; (Kendrick et al., 2012b; Stroncik and Haase, 2004). F/Cl is correlated with K/Cl in the Pitcairn melts.

Fig 11

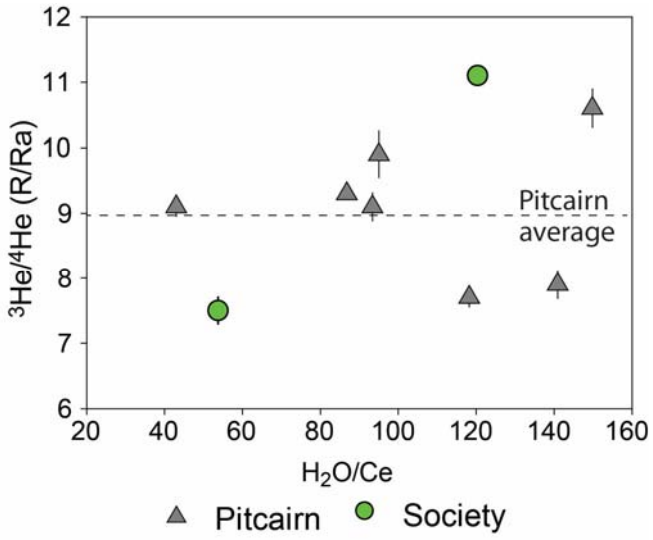

Fig 11. $^3He/^4He$ (R/Ra) versus H_2O/Ce for Pitcairn and Society samples containing $>10^{-7}$ cm^3 STP/g ^4He (Tables 1 and 2; Staudacher and Allegre, 1989; Honda and Woodhead, 2005). Note that Pitcairn samples have an average $^3He/^4He$ of 9 R/Ra that is similar to MORB (Graham, 2002), and that $^3He/^4He$ is not correlated with H_2O/Ce. The $^3He/^4He$ ratios are given relative to the atmospheric value of 1.39×10^{-6}.